Pontifícia Universidade Católica
do Rio de Janeiro

Guilherme Coelho Gomes Barros

Stress Recovery in the Finite Element Method Considering Linearly Dependent Strain Constraints

Tese de Doutorado

Thesis presented to the Programa de Pós–graduação em Engenharia Civil of PUC-Rio in partial fulfillment of the requirements for the degree of Doutor em Engenharia Civil.

Advisor: Prof. Luiz Fernando Martha

Rio de Janeiro
September 2019

Pontifícia Universidade Católica
do Rio de Janeiro

Guilherme Coelho Gomes Barros

Stress Recovery in the Finite Element Method Considering Linearly Dependent Strain Constraints

Thesis presented to the Programa de Pós–graduação em Engenharia Civil of PUC-Rio in partial fulfillment of the requirements for the degree of Doutor em Engenharia Civil. Approved by the Examination Committee:

Prof. Luiz Fernando Martha
Advisor
Departamento de Engenharia Civil e Ambiental – PUC-Rio

Prof. Ivan Fábio Mota de Menezes
Pontifícia Universidade Católica do Rio de Janeiro – PUC-Rio

Prof. Ney Augusto Dumont
Pontifícia Universidade Católica do Rio de Janeiro – PUC-Rio

Prof. André Maués Brabo Pereira
UFF

Prof. Evandro Parente Júnior
UFC

Rio de Janeiro, September 20th, 2019

Guilherme Coelho Gomes Barros

The author graduated in Civil Engineering from Universidade Federal Fluminense – UFF – in 2014 and obtained the title of Master of Science from the Pontifical Catholic University of Rio de Janeiro – PUC-Rio – in 2017.

Bibliographic data

Barros, Guilherme Coelho Gomes

Stress Recovery in the Finite Element Method Considering Linearly Dependent Strain Constraints / Guilherme Coelho Gomes Barros; advisor: Luiz Fernando Martha. – 2019.

60 f: il. color. ; 30 cm

Tese (doutorado) - Pontifícia Universidade Católica do Rio de Janeiro, Departamento de Engenharia Civil e Ambiental, 2019.

Inclui bibliografia

1. Engenharia Civil – Teses. 2. Restrições de Deformação. 3. Restrições Linearmente Dependentes. 4. Recuperação de Tensão. I. Martha, Luiz Fernando. II. Pontifícia Universidade Católica do Rio de Janeiro. Departamento de Engenharia Civil e Ambiental. III. Título.

CDD: 624

To my grandmothers Estela and Therezinha.

Acknowledgments

Firstly, I would like to thank my mother, Evelyn, and my father, Aylton, for guiding me through each step of the way. I owe you everything I have accomplished.

I would also like to thank my siblings Marcelo, Marjorie, Thaís and Thiago for each laugh we shared.

Additionally, I would like to thank my grandmothers Estela and Therezinha, for your loving and caring hearts.

I'm also thankful for my teachers and professors who helped me from basics until calculus of variations, specially Deane Roehl, Paulo Gonçalves, Ney Dumont, Raul Rosas and Ivan Menezes from PUC-Rio.

Additionally, I would like to thank my undergraduate advisor André Pereira for teaching me everything you did, for believing that an undergraduate student could learn all of those advanced subjects, and for our lifelong partnership.

I am also very grateful for having had the opportunity of meeting Luiz Eloy Vaz, who not only taught me mathematical programming and limit analysis, but also represents an example of humbleness and passion for engineering.

Among the professors I had the honor of learning from, I would like to thank my advisor in this work, Luiz Fernando. Thank you for your wise guidance and great patience. I am looking forward to continue working with you.

Moreover, I thank my friend Hugo for all the support he gave me opening the doors of his own house, helping me save several hours spent on traffic, and for all the deep and productive discussions.

Lastly, I would like to thank the National Council for Scientific and Technological Development (CNPq) for the support on the development of this work.

This study was financed in part by the Coordenação de Aperfeiçoamento de Pessoal de Nível Superior - Brasil (CAPES) - Finance Code 001.

Abstract

Barros, Guilherme Coelho Gomes; Martha, Luiz Fernando (Advisor). **Stress Recovery in the Finite Element Method Considering Linearly Dependent Strain Constraints**. Rio de Janeiro, 2019. 60p. Tese de Doutorado – Departamento de Engenharia Civil e Ambiental, Pontifícia Universidade Católica do Rio de Janeiro.

In this work a stress recovery procedure for linearly dependent strain constrained finite element models is presented. Strain constraints arise in several applications such as modeling incompressible materials, inextensible and rigid frame elements. The formulation proposed in this work allows for the treatment of any sort of strain constraint. These constraints are incorporated into the governing equations of the model through the addition of Lagrange multipliers to the total potential energy. A simple mathematical programming problem arises from the discretisation of this modified functional. However, the presence of linearly dependent constraints makes this problem infeasible. The displacements that satisfy the governing equations can be found replacing the constraint matrix by its reduced row echelon form. Nonetheless, this replacement alters the physical meaning and the dimension of the Lagrange multipliers vector space, which are crucial for satisfying the original equilibrium equations and, consequently, to determine the stress field of the model. Hence, this work presents a methodology to recover the Lagrange multipliers of the original problem based on the difference of nodal forces between the constrained and the unconstrained models. In addition, the calculation of the stress field follows from the variation of the modified functional. Several numerical examples are presented to demonstrate the generic characteristic of the proposed methodology and its accuracy. In conclusions, the elastic parameters of the unconstrained model plays an important role on the stress field, and they should be chosen as close as possible to the values that satisfy the constraints.

Keywords

Strain constraints; Linearly dependent constraints; Stress Recovery.

Resumo

Barros, Guilherme Coelho Gomes; Martha, Luiz Fernando. **Recuperação de Tensões no Método dos Elementos Finitos com Restrições de Deformação Linearmente Dependentes**. Rio de Janeiro, 2019. 60p. Tese de Doutorado – Departamento de Engenharia Civil e Ambiental, Pontifícia Universidade Católica do Rio de Janeiro.

Neste trabalho, é apresentada uma metodologia para a análise de modelos de elementos finitos com restrições de deformações linearmente dependentes. Restrições de deformações aparecem em diversas aplicações, como modelagem de materiais incompressíveis e consideração de elementos de pórticos inextensíveis e rígidos. A formulação proposta neste trabalho permite que quaisquer restrições sejam impostas às deformações. Tais restrições são incorporadas às equações que governam o modelo através de multiplicadores de Lagrange adicionados ao princípio da mínima energia potencial total. A discretização desse funcional leva a um problema de programação matemática de simples resolução. Entretanto, a presença de restrições linearmente dependentes torna esse problema impossível. Os deslocamentos que satisfazem às equações do modelo podem ser encontrados substituindo a matriz de restrições por sua versão escalonada. Todavia, essa substituição altera o significado físico e a dimensão do campo vetorial dos multiplicadores de Lagrange, e os multiplicadores de Lagrange do problema original são necessários para atender às equações originais de equilíbrio e, consequentemente, para determinar o campo de tensões do modelo. Dessa forma, é apresentada neste trabalho uma metodologia para recuperar os multiplicadores de Lagrange do problema original baseado na minimização da diferença entre as forças nodais do modelo com restrições e as do modelo sem restrições. Ademais, é apresentada a formulação para a determinação do campo de tensões baseado na variação do funcional modificado. Diversos modelos, tanto contínuos, quanto reticulados, foram analisados e pôde-se constatar a eficiência e precisão da formulação proposta. Também foi notada a influência dos parâmetros elásticos da solução sem restrições no campo de tensões do modelo com restrições. Logo, concluiu-se que esses parâmetros devem ser tão próximos quanto possível àqueles que atendem às restrições.

Palavras-chave

Restrições de Deformação; Restrições Linearmente Dependentes; Recuperação de Tensão.

Table of contents

List of figures

"Knowledge is like a sphere, the greater its volume, the larger its contact with the unknown."

Blaise Pascal, *quote.*

1
Introduction

Linear constraints involving a set of degrees of freedom (dof) associated with different nodes, generally known as multipoint constraints, can be used in structural analysis to model rigid links, diaphragm constraints and skewed supports, join incompatible meshes, and impose cyclic symmetry, among other applications. Thus, the capacity to properly handle linear constraints is an essential part of finite element (FE) software.

Strain constraints are a special case of multipoint constraints because the constraints are written in terms of strain primarily and then written in terms of displacements through finite element approximation. Direct multipoint constraints, on the other hand, are written in terms of displacements directly. Strain constraints are particularly important since the stresses within constrained elements are a matter of interest for the analysis.

Strain constraints are useful in the analysis of framed structures with inextensible and rigid members, i.e., bars without axial and bending strains, respectively. Rigid members can be used in practical applications to model stiff floor systems (rigid diaphragm constraint). In addition, inextensible members may be useful in educational software, since they allow a comparison with results obtained by the classical methods for analysis of statically indeterminate structures that neglect member axial deformation.

The formulation presented in this work allows for a general treatment of strain constrained finite element. Therefore, the aforementioned problems and less commonly practical ones, such as distortion-free elements, rigid finite elements in continuum media, axial-only finite elements, and others are all modeled within the same framework.

The three main approaches to constraint handling are: transformation, penalty function and Lagrange multiplier methods (COOK et al., 2002; FELIPPA, 2017; ZIENKIEWICZ; TAYLOR; ZHU, 2013; BARLOW, 1982; MARTÍN; BENAVENT-CLIMENT; GALLEGO, 2010). The transformation methods, also known as master-slave elimination, use each constraint to eliminate one equilibrium equation, reducing the number of degrees of freedom (DOFs). Since they generate exact results and reduce the number of equations, several different transformation methods have been proposed in the literature (CURISKIS; VALLIAPPAN, 1978; ABEL; SHEPHARD, 1979; WEBB, 1990). However, this approach is difficult to implement for the strain constraint case, due to the complexity of choosing the master DOFs for general

constraints, especially when the same DOF appears in several constraints (FELIPPA, 2017). Moreover, the transformations applied to the equilibrium equations can increase the bandwidth and skyline of the stiffness matrix, increasing the computational cost (BARLOW, 1982). In addition, the main drawback of this approach is that the resulting solution may violate equilibrium conditions (COOK et al., 2002). Hence, the calculated stress may not be in equilibrium with applied forces.

The penalty method can be developed using the so-called Courant quadratic penalty function (FELIPPA, 2017). The penalty function for each constraint is multiplied by a penalty factor (or weight) and the resulting "penalty energy" is added to the total potential energy. Minimization of this augmented energy results in a system of equations including the effect of constraints, but with the same size of the original system. As the penalty factor increases, constraint violation decreases (COOK et al., 2002; FELIPPA, 2017).

This approach can easily handle linearly dependent constraints. In addition, the increase in computational cost is negligible for strain constraints, since it does not affect the size and sparseness of the stiffness matrix. On the other hand, as the penalty factor increases, the stiffness matrix becomes increasingly ill-conditioned, leading to large solutions errors. Some approaches have been proposed to find the best penalty factor that minimizes the total error (FELIPPA, 2017; NOUR-OMID; WRIGGERS, 1987; FELIPPA, 1977). However, the total error cannot be lowered beyond a threshold value (FELIPPA, 2017), which depends on the conditioning of the original (i.e. unconstrained) stiffness matrix.

The Lagrange multiplier method is based on the minimization of the total potential energy with equality constraints (COOK et al., 2002; FELIPPA, 2017; MARTÍN; BENAVENT-CLIMENT; GALLEGO, 2010; HOULSBY; LIU; AUGARDE, 2000; DUBOIS-PÈLERIN; PEGON, 1998) and has a solid mathematical basis on the optimization theory (MEYER, 2000). This approach increases the number of variables and does not have a unique solution in the case of linearly dependent constraints. However, it leads to exact results, can be easily extended to nonlinear problems, and requires no parameters, as in the penalty function approach, and no external data requirement, as in the transformation approach.

This work presents a general treatment of strain constraints in the FE analysis using the Lagrange multipliers formulation. The additional variables needed for the solution, the Lagrange multipliers, are found crucial in the determination of element stresses. Therefore, they may not be seen as additional

computational cost but as important variable for accurate analysis.

The handling of linearly dependent constraints is thoroughly discussed in this work, in both physical and mathematical terms, since this issue has been overlooked in the literature in the context of strain constrained finite elements. A reduced row echelon form (rref) of the constraint matrix is used to eliminate the redundant constraints and the Lagrange multipliers are obtained augmenting the problem with the kernel of the constraint matrix. Since linearly dependent strain constraints of a FE model results in infinite solutions for corner forces, in this work a novel procedure is proposed to find an unique solution. Such solution is achieved minimizing the difference between the corner forces of the constrained and the unconstrained models. Finally, the accuracy and robustness of the proposed treatment is assessed using a set of numerical examples.

This work is organized in eight major chapters. Chapter 3 presents the proposed Lagrange formulation applied to solving finite element models considering strain constraints. It also shows how to handle linearly dependent constraints in order to make the solution for displacement unique. The basis for that is the formulation and solution of a reduced problem, instead of the original one. Chapter 4 describes how to determine the Lagrange multipliers of the original problem based on the Lagrange multipliers of the reduced problem. The Lagrange multipliers of the original problem are fundamental for the calculation of stresses, as detailed in Chapter 5. Chapter 6 Describes the formulation of stiffness and constraint equations for frame elements, considering axial and bending behavior. It presents the basics of this type of analysis and then two possible approaches: the direct finite element approach, and the structural matrix analysis approach. Also, it presents the matrix formulation for local strain constraints, describes the assemblage of the local constraints to the global solution, and addresses the detection of linearly dependent constraints on simple frames for elucidation purpose. Chapter 7 presents several examples of two-dimensional beam and frame models with inextensible or rigid members to assess the accuracy and robustness of the proposed formulation. Finally, Chapter 8 states some concluding remarks about the proposed general treatment for rigid and inextensible members within matrix structural analysis.

2
Formulation of Constrained Model

The minimum total potential energy principle states that the structural response of a elastic body subjected to conservative forces is given by the deformed shape that minimizes the body's total potential energy, given by,

$$\Pi = U + V\,, \tag{2-1}$$

where, V is the potential energy of external loads, given by

$$V = -\int_{\Omega} \boldsymbol{u}^{\mathsf{T}}\boldsymbol{b}\,\mathrm{d}\Omega - \int_{\Gamma} \boldsymbol{u}^{\mathsf{T}}\boldsymbol{t}\,\mathrm{d}\Gamma\,, \tag{2-2}$$

where $\boldsymbol{u}$ are the displacements, $\boldsymbol{b}$ are the body forces, and $\boldsymbol{t}$ are tractions on the boundary. Additionally, U is the strain energy, given by

$$U = \int_{\Omega}\int \boldsymbol{\sigma} d\boldsymbol{\epsilon}\,\mathrm{d}\Omega\,, \tag{2-3}$$

where $\boldsymbol{\epsilon}$ and $\boldsymbol{\sigma}$ are the strain and stress fields, respectively. The constitutive equation that relates these two fields are given by

$$\boldsymbol{\sigma} = \boldsymbol{D}\boldsymbol{\epsilon}\,, \tag{2-4}$$

in which $\boldsymbol{D}$ is the constitutive matrix. Substituting equation (2-4) into equation (2-3) one may find,

$$U = \int_{\Omega} \frac{1}{2}\boldsymbol{\epsilon}^{\mathsf{T}}\boldsymbol{D}\boldsymbol{\epsilon}\,\mathrm{d}\Omega\,. \tag{2-5}$$

Substituting equations (2-2) and (2-5) into equation (2-1) one may find

$$\Pi = \int_{\Omega} \frac{1}{2}\boldsymbol{\epsilon}^{\mathsf{T}}\boldsymbol{D}\boldsymbol{\epsilon}\,\mathrm{d}\Omega - \int_{\Omega} \boldsymbol{u}^{\mathsf{T}}\boldsymbol{b}\,\mathrm{d}\Omega - \int_{\Gamma} \boldsymbol{u}^{\mathsf{T}}\boldsymbol{t}\,\mathrm{d}\Gamma\,. \tag{2-6}$$

When strain constraints are added to the model, one additional equation must hold:

$$\boldsymbol{A}\boldsymbol{\epsilon} = \boldsymbol{e}\,, \tag{2-7}$$

in which $\boldsymbol{A}$ and $\boldsymbol{e}$ are constant, allowing a constraints on the linear combination of strains only. The minimum total potential energy principle is then rewritten as a new functional that incorporates the constraints (COOK et al., 2002; ZIENKIEWICZ; TAYLOR; ZHU, 2013; BATHE, 1996). This new functional is defined as

$$\widetilde{\Pi} = \Pi + \int_{\Omega} \boldsymbol{\gamma}^{\mathsf{T}}\left(\boldsymbol{A}\boldsymbol{\epsilon} - \boldsymbol{e}\right)\mathrm{d}\Omega\,, \tag{2-8}$$

in which, $\boldsymbol{\gamma}$ is a vector function known as Lagrange multipliers. This new functional is hereinafter referred to as generalized potential energy.

An analytical solution of equation (2-8) is a structural response that minimizes the total potential energy and meet the imposed constraints. However, analytical solutions are only available to a limited number of examples. Therefore, instead of seeking analytical solutions for that problem, this work presents how to formulate and determine approximate solutions through the Finite Element Method.

Introducing the displacement interpolation as in any finite elements formulation,

$$\boldsymbol{u} = \boldsymbol{\Phi}\boldsymbol{d}\,, \tag{2-9}$$

in which, $\boldsymbol{\Phi}$ is the interpolation matrix containing shape functions and $\boldsymbol{d}$ are nodal displacements. The strain is then given by

$$\boldsymbol{\epsilon} = \boldsymbol{\nabla}\boldsymbol{u}\,, \tag{2-10}$$

in which, $\boldsymbol{\nabla}$ is the differential operator of mechanics. The kinematic relationship between the strain vector $\boldsymbol{\epsilon}$ and the nodal displacements vector $\boldsymbol{d}$ is obtained substituting equation (2-9) into equation (2-10) as

$$\boldsymbol{\epsilon} = \boldsymbol{\nabla}\boldsymbol{\Phi}\boldsymbol{d} = \boldsymbol{B}\boldsymbol{d}\,, \tag{2-11}$$

in which the $\boldsymbol{B}$ matrix, also known as compatibility matrix, is given by $\boldsymbol{B} = \boldsymbol{\nabla}\boldsymbol{\Phi}$, the derivatives of the shape functions.

Analogously to the displacement interpolation, when seeking approximated solutions to constrained problems, the Lagrange multiplier function also needs an approximation. Hence, it is defined

$$\boldsymbol{\gamma} = \boldsymbol{G}\boldsymbol{\mu}\,, \tag{2-12}$$

Substituting equation (2-11) into the strain energy, equation (2-5), and equation (2-9) into the potential energy, equation (2-2), one may find the discrete form of the total potential energy

$$\Pi = \frac{1}{2}\boldsymbol{d}^{\mathsf{T}}\int_{\Omega}\boldsymbol{B}^{\mathsf{T}}\boldsymbol{D}\boldsymbol{B}\,\mathrm{d}\Omega\,\boldsymbol{d} - \boldsymbol{d}^{\mathsf{T}}\left(\int_{\Omega}\boldsymbol{\Phi}^{\mathsf{T}}\boldsymbol{b}\,\mathrm{d}\Omega + \int_{\Gamma}\boldsymbol{\Phi}^{\mathsf{T}}\boldsymbol{t}\,\mathrm{d}\Gamma\right)\,, \tag{2-13}$$

or, even further,

$$\Pi = \frac{1}{2}\boldsymbol{d}^{\mathsf{T}}\boldsymbol{K}\boldsymbol{d} - \boldsymbol{d}^{\mathsf{T}}\boldsymbol{f}\,. \tag{2-14}$$

where

$$\boldsymbol{K} = \int_{\Omega}\boldsymbol{B}^{\mathsf{T}}\boldsymbol{D}\boldsymbol{B}\,\mathrm{d}\Omega \tag{2-15}$$

is the stiffness matrix and

$$\boldsymbol{f} = \int_{\Omega} \boldsymbol{\Phi}^{\mathsf{T}} \boldsymbol{b} \, \mathrm{d}\Omega + \int_{\Gamma} \boldsymbol{\Phi}^{\mathsf{T}} \boldsymbol{t} \, \mathrm{d}\Gamma \tag{2-16}$$

are equivalent nodal forces.

In order to formulate a discrete form of the generalized potential energy, the Lagrange multipliers interpolation, equation (2-12), is substituted into equation (2-8). Hence,

$$\widetilde{\Pi} = \Pi + \boldsymbol{\mu}^{\mathsf{T}} \int_{\Omega} \boldsymbol{G}^{\mathsf{T}} \boldsymbol{A} \boldsymbol{B} \, \mathrm{d}\Omega \boldsymbol{d} - \boldsymbol{\mu}^{\mathsf{T}} \int_{\Omega} \boldsymbol{G}^{\mathsf{T}} \boldsymbol{e} \, \mathrm{d}\Omega \,, \tag{2-17}$$

or, even further,

$$\widetilde{\Pi} = \Pi + \boldsymbol{\mu}^{\mathsf{T}} \left(\boldsymbol{C} \boldsymbol{d} - \widetilde{\boldsymbol{q}} \right) \,, \tag{2-18}$$

where

$$\boldsymbol{C} = \int_{\Omega} \boldsymbol{G}^{\mathsf{T}} \boldsymbol{A} \boldsymbol{B} \, \mathrm{d}\Omega \tag{2-19}$$

and

$$\widetilde{\boldsymbol{q}} = \int_{\Omega} \boldsymbol{G}^{\mathsf{T}} \boldsymbol{e} \, \mathrm{d}\Omega \tag{2-20}$$

are the discretized constraint matrix and vector, respectively.

Since the shape functions on FEM are defined using local support they are only valid within each element. Therefore, to avoid ambiguity the element stiffness and constraint matrices are hereinafter called $\boldsymbol{K}^e$ and $\boldsymbol{C}^e$, respectively, with the superscript e denoting that they refer to the e-th element. The same is then applied to the nodal equivalent force vector and constraint vector, which are hereinafter denoted $\boldsymbol{f}^e$ and $\boldsymbol{q}^e$, respectively.

The global stiffness matrix $\boldsymbol{K}$ is assembled summing up the contributions of each element and applying boundary conditions, as in any FE formulation. Similarly, a global constraint matrix $\boldsymbol{C}$ is assembled from the contribution of $\boldsymbol{C}^e$ matrix of each element. One difference from the assembling of $\boldsymbol{C}$ to the assembling of $\boldsymbol{K}$ deserves special attention: in the assembling of $\boldsymbol{C}$ the terms of $\boldsymbol{C}^e$ are not summed, but simply stacked.

While assembling $\boldsymbol{K}$, the equilibrium of each dof is considered. The stiffnesses of each element contribute when a dof is mobilized. On the other hand, in assembling $\boldsymbol{C}$ the only consideration that has to be taken into account is that all strain constraints must hold disregarding the interaction between elements.

Another worth mentioning aspect on the assembling of the global strain constraint equations is that the procedure of adding the information of known (prescribed) displacement to the right-hand side of the equation holds. Therefore, consider the system of constraint equations regarding all, known and unknown, degrees of freedom,

$$\begin{bmatrix} \boldsymbol{C} & \boldsymbol{C}_s \end{bmatrix} \begin{Bmatrix} \boldsymbol{d} \\ \boldsymbol{d}_s \end{Bmatrix} = \widetilde{\boldsymbol{q}}\,, \tag{2-21}$$

in which, $\boldsymbol{C}_s$ is the constraint matrix regarding known displacements $\boldsymbol{d}_s$ and $\widetilde{\boldsymbol{q}}$ is the global right-hand side constraint vector, obtained by stacking the $\boldsymbol{q}^e$ vector of each element constraint. Thereafter, it is possible to write:

$$\boldsymbol{C}\boldsymbol{d} = \boldsymbol{q}\,, \tag{2-22}$$

in which,

$$\boldsymbol{q} = \widetilde{\boldsymbol{q}} - \boldsymbol{C}_s\boldsymbol{d}_s\,. \tag{2-23}$$

Thereby, substituting equation (2-14) into equation (2-18) and taking into account boundary conditions, one may find the final form of the discrete generalized potential energy,

$$\widetilde{\Pi} = \frac{1}{2}\boldsymbol{d}^{\mathsf{T}}\boldsymbol{K}\boldsymbol{d} - \boldsymbol{d}^{\mathsf{T}}\boldsymbol{f} + \boldsymbol{\mu}^{\mathsf{T}}\left(\boldsymbol{C}\boldsymbol{d} - \boldsymbol{q}\right)\,. \tag{2-24}$$

3
Solution of Constrained Model

The structural response is then obtained minimizing the total potential energy (Π) subjected to the constraints displayed in equation (2-22). Thus,

$$\begin{aligned} \underset{\boldsymbol{d}}{\text{minimize}} \quad & \Pi = \frac{1}{2}\boldsymbol{d}^{\mathsf{T}}\boldsymbol{K}\boldsymbol{d} - \boldsymbol{d}^{\mathsf{T}}\boldsymbol{f}\,, \\ \text{subject to} \quad & \boldsymbol{C}\boldsymbol{d} = \boldsymbol{q}\,, \end{aligned} \tag{3-1}$$

in which, $\boldsymbol{f}$ is the global nodal force vector.

Equation (3-1) is a quadratic programming (QP) problem (NOCEDAL; WRIGHT, 2006). A primal-dual solution is sought in this work, since both the primal and dual variables are necessary for complete structural response. The primal variables are the displacements, while the dual variables are the so-called Lagrange multipliers, that, as demonstrated later in this work, are necessary in the calculation of stresses.

However, the problem in equation (3-1) only has an unique primal-dual solution if the constraint matrix is full row rank. This are often not the case when strain constraints are considered. In statically indeterminate structural systems, linearly dependent constraints commonly appears as exemplified in .

A way around this problem is to use the reduced row echelon form (rref) of the constraint matrix augmented by the constraint vector, taking only the nonzero part. Namely,

$$\text{rref}\left(\begin{bmatrix}\boldsymbol{C} & \boldsymbol{q}\end{bmatrix}\right) = \begin{bmatrix}\boldsymbol{H} & \boldsymbol{p} \\ \underset{\sim}{\boldsymbol{0}} & \boldsymbol{y}\end{bmatrix}\,, \tag{3-2}$$

in which, $\boldsymbol{H}$ is the reduced constraint matrix and $\boldsymbol{p}$ is its corresponding right-hand side vector.

The second set of equations in equation (3-2) contains a all zero matrix, represented by $\underset{\sim}{\boldsymbol{0}}$ and a vector $\boldsymbol{y}$, which writes

$$\underset{\sim}{\boldsymbol{0}}\boldsymbol{d} = \boldsymbol{y}\,. \tag{3-3}$$

Thereby, a solution to equation (3-1) exists if and only if $\boldsymbol{y}$ is identically null. That information may not be clear in equation (2-22), but is easily verified after reducing the system.

After verifying the equality $\boldsymbol{y} = \vec{\boldsymbol{0}}$, equation (3-1) may be rewritten using the reduced constraint matrix as

$$\begin{aligned} \underset{\boldsymbol{d}}{\text{minimize}} \quad & \Pi = \frac{1}{2}\boldsymbol{d}^{\mathsf{T}}\boldsymbol{K}\boldsymbol{d} - \boldsymbol{d}^{\mathsf{T}}\boldsymbol{f}\,, \\ \text{subject to} \quad & \boldsymbol{H}\boldsymbol{d} = \boldsymbol{p}\,, \end{aligned} \tag{3-4}$$

which has an unique primal-dual solution. This solution can be found writing the Lagrangian function associated to equation (3-4) and taking the derivative with respect to the primal and dual variables, $\boldsymbol{d}$ and $\boldsymbol{\lambda}$ respectively (KUHN; TUCKER, 1951),

$$\mathcal{L} = \frac{1}{2}\boldsymbol{d}^{\mathsf{T}}\boldsymbol{K}\boldsymbol{d} - \boldsymbol{d}^{\mathsf{T}}\boldsymbol{f} + \boldsymbol{\lambda}^{\mathsf{T}}\left(\boldsymbol{H}\boldsymbol{d} - \boldsymbol{p}\right)\,, \tag{3-5}$$

in which, $\boldsymbol{\lambda}$ are the Lagrange multipliers of equation (3-4). The Lagrangian function, Equation (3-5), from the field of mathematical programming, is analogous to the discrete generalized potential energy, Equation (2-24). The only exception is that $\boldsymbol{\lambda}$ are the Lagrange multipliers of the reduced constraint system, $\boldsymbol{H}\boldsymbol{d} = \boldsymbol{p}$, and $\boldsymbol{\mu}$ the ones of the original constraint system, $\boldsymbol{C}\boldsymbol{d} = \boldsymbol{q}$.

Taking the derivatives with respect to the primal variables one finds

$$\frac{\partial \mathcal{L}}{\partial \boldsymbol{d}} = \boldsymbol{K}\boldsymbol{d} + \boldsymbol{H}^{\mathsf{T}}\boldsymbol{\lambda} - \boldsymbol{f} = \vec{\boldsymbol{0}}\,, \tag{3-6}$$

which is the equilibrium equation of the constrained model. Thereafter, taking the derivative of the Lagrangian function according to the dual variables one finds

$$\frac{\partial \mathcal{L}}{\partial \boldsymbol{\lambda}} = \boldsymbol{H}\boldsymbol{d} - \boldsymbol{p} = \vec{\boldsymbol{0}}\,, \tag{3-7}$$

which is exactly the constraint in equation (3-4).

The solution sought must simultaneously meet equations (3-6) and (3-7). References (COOK et al., 2002; ZIENKIEWICZ; TAYLOR; ZHU, 2013; BATHE, 1996) present two possible solution schemes for solving one system of equations altogether: direct solution of the system using, for example, Gauss elimination; and penalty functions to enforce constraints. However, the problem with the first scheme is that it does not benefit from the sparse characteristic of the stiffness matrix. In addition, this scheme would modify the implementation of a conventional FE program. On the other hand, the penalty functions scheme may potentially introduce numerical errors (MEYER, 2000), which is demonstrated in a numerical study presented here in the first example of Chapter 7.

The methodology proposed herein avoids these two problems. First, equation (3-6) is solved for $\boldsymbol{d}$

$$\boldsymbol{d} = \boldsymbol{K}^{-1}\left(\boldsymbol{f} - \boldsymbol{H}^{\mathsf{T}}\boldsymbol{\lambda}\right) = \boldsymbol{d}_u - \boldsymbol{L}\boldsymbol{\lambda}\,, \tag{3-8}$$

in which, $\boldsymbol{d}_u = \boldsymbol{K}^{-1}\boldsymbol{f}$ is the solution of the unconstrained model and $\boldsymbol{L} = \boldsymbol{K}^{-1}\boldsymbol{H}^{\mathsf{T}}$. Equation (3-8) holds because the stiffness matrix relating

unrestrained degrees of freedom, is nonsingular. It should be noted that there is no need here to invert the stiffness matrix, a multiple right-hand side system can be solved instead. Then, equation (3-8) is substituted back to equation (3-7) giving

$$\boldsymbol{HL\lambda} = \boldsymbol{Hd}_u - \boldsymbol{p}\,. \tag{3-9}$$

Matrix $\boldsymbol{HL} = \boldsymbol{HK}^{-1}\boldsymbol{H}^{\mathsf{T}}$ is squared and symmetric and is nonsingular since $\boldsymbol{K}$ is nonsingular and $\boldsymbol{H}$ is full row rank. Equation (3-9) is then solved for $\boldsymbol{\lambda}$. The solution is completed by calculating the displacements substituting the Lagrange multipliers back into equation (3-8). If the rref process was not performed, the solution for the Lagrange would not exist, since the resulting matrix would be singular.

The primal solution of equations (3-1) and (3-4) are the same, however the Lagrange multipliers are different in size and physical meaning. Since the Lagrange multipliers of equation (3-1) are needed in the calculation of strains and stresses, a procedure to retrieve this dual solution is presented.

This procedure begins by performing rref in the constraint matrix $\boldsymbol{C}$ augmented by an identity matrix of order equals the number of constraints,

$$\text{rref}\left(\begin{bmatrix}\boldsymbol{C} & \boldsymbol{I}\end{bmatrix}\right) = \begin{bmatrix}\boldsymbol{H} & \boldsymbol{Z} \\ \underset{\sim}{\boldsymbol{0}} & \boldsymbol{S}\end{bmatrix}\,. \tag{3-10}$$

Comparing equations (3-2) and (3-10), it may be noted that

$$\boldsymbol{p} = \boldsymbol{Zq}\,, \tag{3-11}$$

and

$$\boldsymbol{y} = \boldsymbol{Sq}\,. \tag{3-12}$$

One possible solution for the Lagrange multipliers of equation (3-1) $\boldsymbol{\mu}$ is

$$\boldsymbol{\mu} = \boldsymbol{Z}^{\mathsf{T}}\boldsymbol{\lambda}\,. \tag{3-13}$$

However, if $\boldsymbol{C}$ is not full row rank that solution is not unique, and may be seen as a particular solution.

To prove that equation (3-13) actually is a solution for the Lagrange multipliers of equation (3-1) substitute equation (3-11) into equation (3-7), which gives

$$\boldsymbol{Hd} = \boldsymbol{Zq}\,, \tag{3-14}$$

and then substitute equation (2-22) into equation (3-14), finding

$$\boldsymbol{Hd} = \boldsymbol{ZCd}\,, \tag{3-15}$$

which must hold for any $\boldsymbol{d}$, hence

$$\boldsymbol{H}^{\mathsf{T}} = \boldsymbol{C}^{\mathsf{T}}\boldsymbol{Z}^{\mathsf{T}}\,. \tag{3-16}$$

Substituting equation (3-16) into equation (3-6)

$$\boldsymbol{K}\boldsymbol{d} + \boldsymbol{H}^{\mathsf{T}}\boldsymbol{\lambda} = \boldsymbol{f}\,, \tag{3-17}$$

one finds

$$\boldsymbol{K}\boldsymbol{d} + \boldsymbol{C}^{\mathsf{T}}\boldsymbol{Z}^{\mathsf{T}}\boldsymbol{\lambda} = \boldsymbol{f}\,. \tag{3-18}$$

The equilibrium equation found taking the derivative of the Lagrangian function associated with equation (3-1) with respect to the displacements is

$$\boldsymbol{K}\boldsymbol{d} + \boldsymbol{C}^{\mathsf{T}}\boldsymbol{\mu} = \boldsymbol{f}\,. \tag{3-19}$$

Equation (3-13) is found by simple comparison between equations (3-18) and (3-19).

However, equation (3-13) may be augmented by its homogeneous solution, which is any solution that does not interfere in the global equilibrium, equation (3-19). That can be obtained by

$$\boldsymbol{\mu} = \boldsymbol{Z}^{\mathsf{T}}\boldsymbol{\lambda} + \boldsymbol{S}^{\mathsf{T}}\boldsymbol{\alpha}\,. \tag{3-20}$$

It has already been proven that equation (3-13) is a particular solution of the global equilibrium equation (3-19). Now, to prove that $\boldsymbol{\mu} = \boldsymbol{S}^{\mathsf{T}}\boldsymbol{\alpha}$ is a homogeneous solution one should seek to prove that

$$\boldsymbol{C}^{\mathsf{T}}\boldsymbol{S}^{\mathsf{T}}\boldsymbol{\alpha} = \vec{\boldsymbol{0}} \tag{3-21}$$

for any possible value of $\boldsymbol{\alpha}$. That means $\boldsymbol{S}$ is a basis of the null space of matrix $\boldsymbol{C}$ and $\boldsymbol{\alpha}$ produces a linear combination of these vectors, which still lies in the null space. To prove that substitute equation (3-20) into equation (3-19), which furnishes

$$\boldsymbol{C}^{\mathsf{T}}\boldsymbol{Z}^{\mathsf{T}}\boldsymbol{\lambda} + \boldsymbol{C}^{\mathsf{T}}\boldsymbol{S}^{\mathsf{T}}\boldsymbol{\alpha} = \boldsymbol{f} - \boldsymbol{K}\boldsymbol{d}\,, \tag{3-22}$$

which, substituting equation (3-18) gives

$$\boldsymbol{C}^{\mathsf{T}}\boldsymbol{Z}^{\mathsf{T}}\boldsymbol{\lambda} + \boldsymbol{C}^{\mathsf{T}}\boldsymbol{S}^{\mathsf{T}}\boldsymbol{\alpha} = \boldsymbol{C}^{\mathsf{T}}\boldsymbol{Z}^{\mathsf{T}}\boldsymbol{\lambda}\,, \tag{3-23}$$

therefore, equation (3-21) must hold.

The solution of displacement is already defined by equation (3-8) however, the complete solution, in terms of strain and stress still depends on the Lagrange multipliers $\boldsymbol{\mu}$ of the original problem equation (3-1). Equation (3-20) results in infinite possible solutions for $\boldsymbol{\mu}$. As demonstrated, any choice will not interfere in the global equilibrium, however the stress distribution is severally affected by this choice. Hence, a procedure for an unique determination of $\boldsymbol{\mu}$ is presented in Chapter 4.

4
Determination of the Lagrange Multipliers

There are infinity possible solutions for the Lagrange multipliers $\boldsymbol{\mu}$ of the original problem of minimizing the total potential energy, subjected to strain constraints, equation (3-1). All of these solutions meets the global equilibrium equation, equation (3-19). Each of them produces a different distribution of stresses, as demonstrated in Chapter 5.

Therefore, infinity stress distribution are available. There is mainly the case in statically indeterminate systems when only equilibrium equations are available. Which is exactly the case when strain constraints are applied since they reduce the number of available compatibility equations.

The procedure introduced in this work consists of finding the stress distribution that resembles as much as possible the stress distribution of the unconstrained model. In other words, the elastic stresses calculated from the displacement vector $\boldsymbol{d}_u$, disregarding constraints.

To achieve this goal, it is minimized the quadratic difference between the corner forces of the unconstrained model

$$\boldsymbol{f}_u^e = \boldsymbol{K}^e \boldsymbol{d}_u^e \,, \tag{4-1}$$

and the corner forces of the constrained model

$$\boldsymbol{f}^e = \boldsymbol{K}^e \boldsymbol{d}^e + \boldsymbol{C}^{e\mathsf{T}} \boldsymbol{\mu}^e \,. \tag{4-2}$$

In equation (4-1) $\boldsymbol{d}_u^e$ is the unconstrained element displacement vector retrieved from the global unconstrained displacement vector $\boldsymbol{d}_u$. On the other hand, in equation (4-2) $\boldsymbol{d}^e$ is the element displacement vector retrieved from the global displacement vector $\boldsymbol{d}$ and $\boldsymbol{\mu}^e$ are the Lagrange multipliers associated with element's strain constraint, which is retrieved from $\boldsymbol{\mu}$.

Therefore the difference minimization process aforementioned is described as

$$\underset{\boldsymbol{\alpha}}{\text{minimize}} \quad \mathcal{F} = \sum_e \left(\boldsymbol{f}^e - \boldsymbol{f}_u^e\right)^{\mathsf{T}} \left(\boldsymbol{f}^e - \boldsymbol{f}_u^e\right) \quad . \tag{4-3}$$

Note that the only unknowns in equation (4-3) are the homogeneous solution parameters $\boldsymbol{\alpha}$. That can be seen by substitution of equations (3-20), (4-1) and (4-2) into equation (4-3).

Retrieving $\boldsymbol{\mu}^e$ from $\boldsymbol{\mu}$ with unknown vector $\boldsymbol{\alpha}$, may be written as

$$\boldsymbol{\mu}^e = \boldsymbol{Z}^{e\mathsf{T}} \boldsymbol{\lambda} + \boldsymbol{S}^{e\mathsf{T}} \boldsymbol{\alpha} \,, \tag{4-4}$$

in which, $\boldsymbol{Z}^e$ and $\boldsymbol{S}^e$ are obtained retrieving the rows corresponding to

element's constraints from $\boldsymbol{Z}$ and $\boldsymbol{S}$, respectively. Equation (4-4) is equivalent to equation (3-20) at element level.

Gathering equations (4-1), (4-2) and (4-4), the term $\boldsymbol{f}^e - \boldsymbol{f}_u^e$ in equation (4-3) may be written as

$$\boldsymbol{f}^e - \boldsymbol{f}_u^e = \boldsymbol{K}^e \left(\boldsymbol{d}^e - \boldsymbol{d}_u^e\right) + \boldsymbol{C}^{e\mathsf{T}} \boldsymbol{Z}^{e\mathsf{T}} \boldsymbol{\lambda} + \boldsymbol{C}^{e\mathsf{T}} \boldsymbol{S}^{e\mathsf{T}} \boldsymbol{\alpha} \,. \tag{4-5}$$

Note that the only unknown in equation (4-5) is $\boldsymbol{\alpha}$. Therefore, even though the equation being minimized in equation (4-3) may have nine terms only three will appear in the final solution. That happens because the solution is obtained by taking the derivative of $\mathcal{F}$ in equation (4-3) with respect to $\boldsymbol{\alpha}$ to zero. Thus, the derivatives of terms independent of $\boldsymbol{\alpha}$ go to zero.

The solution of $\boldsymbol{\alpha}$, and hence the final solution of $\boldsymbol{\mu}$ is obtained from

$$\frac{d\mathcal{F}}{d\boldsymbol{\alpha}} = \boldsymbol{M}\boldsymbol{\alpha} + \boldsymbol{v} = \vec{\boldsymbol{0}} \,, \tag{4-6}$$

in which,

$$\boldsymbol{M} = \sum_e \left(\boldsymbol{S}^e \boldsymbol{C}^e \boldsymbol{C}^{e\mathsf{T}} \boldsymbol{S}^{e\mathsf{T}}\right) \,, \tag{4-7}$$

and

$$\boldsymbol{v} = \boldsymbol{S}^e \boldsymbol{C}^e \left[\boldsymbol{K}^e \left(\boldsymbol{d}^e - \boldsymbol{d}_u^e\right) + \boldsymbol{C}^{e\mathsf{T}} \boldsymbol{Z}^{e\mathsf{T}} \boldsymbol{\lambda}\right] \,. \tag{4-8}$$

Solving the system of equations in equation (4-6) for $\boldsymbol{\alpha}$ completes the determination of variables in the global equilibrium equation equation (3-19). That solution is obtained through an iterative solver, such as conjugate gradient, since the direct solution may not be available if element strain constraints already contains linear dependency.

For the complete solution of the constrained model, strains and stresses are to be determined. A procedure to obtain these results is presented on Chapter 5. This procedure uses the determined values of $\boldsymbol{d}^e$ and $\boldsymbol{\mu}^e$, from equation (4-4).

5
Stress Recovery

Once the displacements and Lagrange multipliers are determined, strain and stress calculation are the remaining step of analysis. Strains are calculated in the standard manner, by equation (2-11). Since constraints were added into the global solution, these strains fully meet equation (2-7). However, calculation of stresses through elastic relations, equation (2-4), leads to violations of equilibrium relations.

In order to shed lights on this equilibrium violation two explanations are provided. First, considering the global equilibrium equation, equation (3-19), it is clear that the forces written in terms of displacements, term $\boldsymbol{Kd}$, alone does not satisfy the equilibrium equations. Therefore, stresses calculated through the same displacements cannot be in equilibrium with the external forces.

The equilibrium violation may also be glimpsed by a more physical way. Consider for instance an undeformable media being tensioned as depicted in Figure 5.1, being the mesh a single Q4 element. To model this example within the framework presented in this work, using equation (2-7), $\boldsymbol{A}$ is an identity matrix of order three, and $\boldsymbol{e}$ is an all zero vector, of size three as well. The only possible solution for the displacements is to be null. Therefore, all strains are null, and the stress calculated by equation (2-4) would be null, which clearly disagrees with the tension stress state imposed by external loads.

Therefore, the determination of the stress field can be found through the variation of the generalized potential energy, Equation (2-8), which can be extended as

$$\widetilde{\Pi} = \int_{\Omega} \frac{1}{2} \boldsymbol{\epsilon}^{\mathsf{T}} \boldsymbol{D} \boldsymbol{\epsilon} \, \mathrm{d}\Omega - \int_{\Omega} \boldsymbol{u}^{\mathsf{T}} \boldsymbol{b} \, \mathrm{d}\Omega - \int_{\Gamma} \boldsymbol{u}^{\mathsf{T}} \boldsymbol{t} \, \mathrm{d}\Gamma + \int_{\Omega} \boldsymbol{\gamma}^{\mathsf{T}} \left(\boldsymbol{A} \boldsymbol{\epsilon} - \boldsymbol{e} \right) \mathrm{d}\Omega \, . \qquad (5\text{-}1)$$

The variation of this functional can be written as

Figure 5.1: Undeformable media Q4 patch test.

$$\begin{aligned}\delta\widetilde{\Pi} = &\int_{\Omega} \delta\boldsymbol{\epsilon}^{\mathsf{T}} \left(\boldsymbol{D}\boldsymbol{\epsilon} + \boldsymbol{A}^{\mathsf{T}}\boldsymbol{\gamma}\right) \mathrm{d}\Omega - \int_{\Omega} \delta\boldsymbol{u}^{\mathsf{T}}\boldsymbol{b}\,\mathrm{d}\Omega - \int_{\Gamma} \delta\boldsymbol{u}^{\mathsf{T}}\boldsymbol{t}\,\mathrm{d}\Gamma \\ &+ \int_{\Omega} \delta\boldsymbol{\gamma}^{\mathsf{T}} \left(\boldsymbol{A}\boldsymbol{\epsilon} - \boldsymbol{e}\right) \mathrm{d}\Omega\,.\end{aligned} \tag{5-2}$$

It can be seen that the field that performs work on the variation of strains $\delta\boldsymbol{\epsilon}$, better known as the stress field, is given by:

$$\boldsymbol{\sigma} = \boldsymbol{D}\boldsymbol{\epsilon} + \boldsymbol{A}^{\mathsf{T}}\boldsymbol{\gamma}\,. \tag{5-3}$$

6
Frame Elements

The formulation for frame elements may follow the conventional finite element formulation, or may be derived as in the field of structural matrix analysis, using a fundamental system (MCGUIRE; GALLAGHER; ZIEMIAN, 2014). Both formulations lead to the same solution, since the shape functions used satisfy the governing ordinary differential equations, for prismatic members.

In Section 6.1 the governing differential equations are revisited and the shape functions that satisfy them are found. Thereafter, the formulation of stiffness equations using the principle of virtual displacements as in a generic finite element is presented in Section 6.2. Furthermore, the fundamental system of equations and the assemblage of stiffness matrix as in structural matrix analysis is presented in Section 6.3.

6.1
Differential Equations

A prismatic frame member is described according to its local axes x' and y' as illustrated in Figure 6.1. It may be subjected to distributed loads q_x and q_y, as depicted in Figure 6.2. For the member to be in equilibrium, any part of it must be in equilibrium. Therefore, considering the whole member one may find that the nodal forces, in Figure 6.3, must balance the distributed loads. A more valuable equation, however, is found when considering the equilibrium of an infinitesimal element as indicated in Figure 6.4. The axial normal force at the left face is N but in the right face it has an increment due to the presence of axial distributed load q_x. The balance of forces acting on the direction of the x' axis is given by

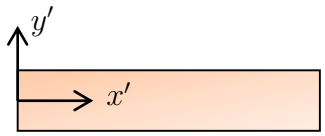

Figure 6.1: Frame member local axes.

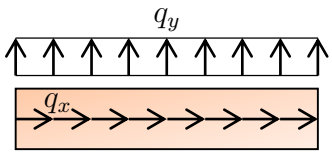

Figure 6.2: Frame member distributed loads.

Figure 6.3: Frame member nodal forces.

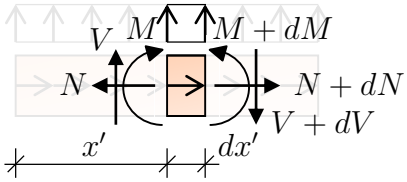

Figure 6.4: Frame member internal forces.

$$\sum F_{x'} = 0 \therefore -N + q_x\, dx' + N + dN = 0\,, \tag{6-1}$$

which gives

$$\frac{dN}{dx'} = -q_x\,. \tag{6-2}$$

Moreover, according to Figure 6.3, the shear force at the left face is V. However, due to the distributed load q_y it is incremented of dV at the right face. Balance according to y' is given by

$$\sum F_{y'} = 0 \therefore V + q_y\, dx' - V - dV = 0\,, \tag{6-3}$$

which equates to

$$\frac{dV}{dx'} = q_y\,. \tag{6-4}$$

Furthermore, the distributed load q_y also causes changes in the bending moment from M at the left face to $M + dM$ at the right face. Balance of moments along z'-axis at point $x' + dx'$ gives

$$\sum M_{z'}^{x'} = 0 \therefore -V\, dx' - M - q_y\,(dx')^2 + M + dM = 0\,, \tag{6-5}$$

neglecting high order terms and isolating V one may find

$$\frac{dM}{dx'} = V\,. \tag{6-6}$$

Substitution of equation (6-6) into equation (6-4) gives

$$\frac{d^2M}{dx'^2} = q_y\,. \tag{6-7}$$

Considering the Bernoulli-Euler beam theory, which states that plane sections taken in the undeformed configuration remains plane and perpendicular to the structure axis as it undergoes deformation, one may find

$$N = EA\epsilon^a_{xx}\,, \tag{6-8}$$

$$M = EI\kappa\,, \tag{6-9}$$

in which, $\epsilon^a_{xx} = \frac{du}{dx'}$ is the axial deformation measured at the element axis, and $\kappa = \frac{d^2v}{dx'^2}$ is the section curvature. Grouping equations (6-8) and (6-9) in matrix form, it can be stated

$$\begin{Bmatrix} N \\ M \end{Bmatrix} = \begin{bmatrix} EA & 0 \\ 0 & EI \end{bmatrix} \begin{Bmatrix} \epsilon^a_{xx} \\ \kappa \end{Bmatrix}. \tag{6-10}$$

Combining equations (6-2) and (6-8) one may find

$$\frac{d^2u}{dx'^2} = -\frac{q_x}{EA}\,, \tag{6-11}$$

and, substituting equation (6-9) into equation (6-7)

$$\frac{d^4v}{dx'^4} = \frac{q_y}{EI}\,. \tag{6-12}$$

Equations (6-11) and (6-12) are the governing differential equations of a frame member. As in any differential equation, the solution is given by the summation of a particular and homogeneous solution. The homogeneous solution of the axial problem may be given by a polynomial of order 1,

$$u\left(x'\right) = ax' + b\,, \tag{6-13}$$

whose second derivative vanishes. The solution is more often written in terms of nodal displacements rather than constants a and b. The transformation of constants may be found through

$$u\left(x' = 0\right) = u_1\,, \tag{6-14}$$

$$u\left(x' = L\right) = u_2\,, \tag{6-15}$$

which gives

$$u\left(x'\right) = \phi_1\left(x'\right)u_1 + \phi_2\left(x'\right)u_2\,, \tag{6-16}$$

in which,

$$\phi_1\left(x'\right) = 1 - \frac{x'}{L}\,, \tag{6-17}$$

$$\phi_2\left(x'\right) = \frac{x'}{L}\,. \tag{6-18}$$

Functions ϕ_1 and ϕ_2 are know as shape functions.

Following the same procedure for equation (6-12) gives

$$v\left(x'\right) = \phi_3\left(x'\right)v_1 + \phi_4\left(x'\right)\theta_1 + \phi_5\left(x'\right)v_2 + \phi_6\left(x'\right)\theta_2\,, \tag{6-19}$$

in which,

$$\phi_3(x') = 1 - 3\left(\frac{x'}{L}\right)^2 + 2\left(\frac{x'}{L}\right)^3 , \tag{6-20}$$

$$\phi_4(x') = x'\left(1 - \frac{x'}{L}\right)^2 , \tag{6-21}$$

$$\phi_5(x') = 3\left(\frac{x'}{L}\right)^2 - 2\left(\frac{x'}{L}\right)^3 , \tag{6-22}$$

$$\phi_6(x') = x'\left[\left(\frac{x'}{L}\right)^2 - \frac{x'}{L}\right] \tag{6-23}$$

6.2 Finite Element Formulation

The finite element approach for frame elements is rooted at the definition of the displacement fields as a function of nodal displacements interpolated by shape functions, as in equation (2-9). Using the shape functions derived in Section 6.1 it is stated that

$$\boldsymbol{u} = \begin{Bmatrix} u \\ v \end{Bmatrix} , \tag{6-24}$$

$$\boldsymbol{d} = \begin{Bmatrix} u_1 \\ v_1 \\ \theta_1 \\ u_2 \\ v_2 \\ \theta_2 \end{Bmatrix} , \tag{6-25}$$

$$\boldsymbol{\Phi} = \begin{bmatrix} \phi_1 & 0 & 0 & \phi_2 & 0 & 0 \\ 0 & \phi_3 & \phi_4 & 0 & \phi_5 & \phi_6 \end{bmatrix} . \tag{6-26}$$

The generic differential operator $\boldsymbol{\nabla}$, in equation (2-10), is defined for frame elements as

$$\boldsymbol{\nabla} = \begin{bmatrix} \frac{d}{dx'} & 0 \\ 0 & \frac{d^2}{dx'^2} \end{bmatrix} , \tag{6-27}$$

which transform the displacement field to the strains field

$$\boldsymbol{\epsilon} = \begin{Bmatrix} \epsilon^a_{xx} \\ \kappa \end{Bmatrix} . \tag{6-28}$$

The resulting $\boldsymbol{B}$ matrix, equation (2-11), is

$$\boldsymbol{B} = \begin{bmatrix} -\frac{1}{L} & 0 & 0 & \frac{1}{L} & 0 & 0 \\ 0 & -\frac{6\,(L-2\,x')}{L^3} & -\frac{2\,(2\,L-3\,x')}{L^2} & 0 & \frac{6\,(L-2\,x')}{L^3} & -\frac{2\,(L-3\,x')}{L^2} \end{bmatrix} . \tag{6-29}$$

Comparing equations (2-4) and (6-10) it can be seen that for frame elements

$$\boldsymbol{\sigma} = \begin{Bmatrix} N \\ M \end{Bmatrix}, \tag{6-30}$$

$$\boldsymbol{D} = \begin{bmatrix} EA & 0 \\ 0 & EI \end{bmatrix}, \tag{6-31}$$

and $\boldsymbol{\epsilon}$ is given by equation (6-28). Thereby, performing the integration on equation (2-15) gives the well known frame stiffness matrix,

$$\boldsymbol{K} = \begin{bmatrix} \frac{EA}{L} & 0 & 0 & -\frac{EA}{L} & 0 & 0 \\ 0 & \frac{12EI}{L^3} & \frac{6EI}{L^2} & 0 & -\frac{12EI}{L^3} & \frac{6EI}{L^2} \\ 0 & \frac{6EI}{L^2} & \frac{4EI}{L} & 0 & -\frac{6EI}{L^2} & \frac{2EI}{L} \\ -\frac{EA}{L} & 0 & 0 & \frac{EA}{L} & 0 & 0 \\ 0 & -\frac{12EI}{L^3} & -\frac{6EI}{L^2} & 0 & \frac{12EI}{L^3} & -\frac{6EI}{L^2} \\ 0 & \frac{6EI}{L^2} & \frac{2EI}{L} & 0 & -\frac{6EI}{L^2} & \frac{4EI}{L} \end{bmatrix} \tag{6-32}$$

It is considered in the sequel the introduction of strain constraints, as per the framework shown in Chapter 2, to model inextensible and rigid member behavior. Consequently, the inextensible behavior can be modeled assuming

$$\boldsymbol{A} = \begin{bmatrix} 1 & 0 \end{bmatrix}, \tag{6-33}$$

and

$$\boldsymbol{e} = \begin{Bmatrix} 0 \end{Bmatrix}, \tag{6-34}$$

once,

$$\boldsymbol{A\epsilon} = \begin{bmatrix} 1 & 0 \end{bmatrix} \begin{Bmatrix} \epsilon^a_{xx} \\ \kappa \end{Bmatrix} = \epsilon^a_{xx} = 0 = \boldsymbol{e}\,. \tag{6-35}$$

Substituting it back into equation (2-19) gives

$$\boldsymbol{C} = \int_0^L \boldsymbol{G}^{\mathsf{T}}\, \mathrm{d}x' \begin{bmatrix} -\frac{1}{L} & 0 & 0 & \frac{1}{L} & 0 & 0 \end{bmatrix} \boldsymbol{d}\,. \tag{6-36}$$

The distribution of normal stresses in a inextensible member is known to be constant, therefore, the Lagrange multiplier function γ is equal to the scalar μ. In other words, the interpolation matrix $\boldsymbol{G}$ is a constant given by

$$\boldsymbol{G} = \begin{bmatrix} 1 \end{bmatrix}. \tag{6-37}$$

Substituting it back into equation (6-36) gives

$$\boldsymbol{C} = \begin{bmatrix} -1 & 0 & 0 & 1 & 0 & 0 \end{bmatrix}. \tag{6-38}$$

Theoretically, the discretization of the Lagrange multiplier function, hence the axial force distribution, can be enriched. However, any interpolation function added will only generate different constants after integration, *i.e.*, will merely generate a linearly dependent constraint.

On the other hand, rigid behavior may be achieved taking

$$\boldsymbol{A} = \begin{bmatrix} 1 & 0 \\ 0 & 1 \end{bmatrix} , \tag{6-39}$$

and

$$\boldsymbol{e} = \begin{Bmatrix} 0 \\ 0 \end{Bmatrix} , \tag{6-40}$$

since,

$$\boldsymbol{A\epsilon} = \begin{bmatrix} 1 & 0 \\ 0 & 1 \end{bmatrix} \begin{Bmatrix} \epsilon^a_{xx} \\ \kappa \end{Bmatrix} = \begin{Bmatrix} \epsilon^a_{xx} \\ \kappa \end{Bmatrix} = \begin{Bmatrix} 0 \\ 0 \end{Bmatrix} = \boldsymbol{e} . \tag{6-41}$$

Noting that, since the member is rigid, all the strain are zero, the first term in the calculation of stresses, Equation (5-3), is null. Therefore, the stress field, axial force and bending moment, is determined through the Lagrange multipliers only. In addition, since $\boldsymbol{A}$ is an identity matrix, $\boldsymbol{\sigma} = \boldsymbol{G\mu}$, hence the choice of interpolation function translates directly to the distribution of forces within the member.

To shed some lights into that, it is first assumed that the Lagrange multiplier function is constant for both constraints, $\epsilon^a_{xx} = 0$ and $\kappa = 0$. Which translates to assuming that the axial force and bending moment are constant over the member. In such case one may write,

$$\boldsymbol{G} = \begin{bmatrix} 1 & 0 \\ 0 & 1 \end{bmatrix} , \tag{6-42}$$

which gives, substituting back into equation (2-19),

$$\boldsymbol{C} = \begin{bmatrix} -1 & 0 & 0 & 1 & 0 & 0 \\ 0 & 0 & -1 & 0 & 0 & 1 \end{bmatrix} . \tag{6-43}$$

It can be seen that the resulting constraint matrix imposes that the axial strain is equal to zero and that the rotations of both ends should be equal. Although, this is a necessary condition, it is still not enough to impose rigid behavior. Therefore, a higher order of interpolation shall be used in the Lagrange multipliers to impose rigid behavior properly. Thus, adding a linear term one may write

$$\boldsymbol{G} = \begin{bmatrix} 1 & 0 & 0 \\ 0 & 1 & x' \end{bmatrix} , \tag{6-44}$$

which gives, substituting back into equation (2-19),

$$\boldsymbol{C} = \begin{bmatrix} -1 & 0 & 0 & 1 & 0 & 0 \\ 0 & 0 & -1 & 0 & 0 & 1 \\ 0 & 1 & 0 & 0 & -1 & L \end{bmatrix} , \tag{6-45}$$

in which is worth noticing that a new, linearly independent constraint is found. The new constraint in the third line of the constraint matrix bonds the rotation of the end node with the transverse displacements of the member. Analyzing

the impact of adding a linear upon the distribution of internal forces, it may be stated from Equation (5-3), that the first discrete Lagrange multiplier is equivalent to constant axial force on the member. In addition, the bending moment will be given by

$$M = \mu_2 + x'\mu_3 \,. \tag{6-46}$$

It can be seen that μ_2 corresponds to the bending moment at the beginning of the member while μ_3 corresponds to the constant shear force over the member.

The equations in Equation (6-45) are enough to enforce rigid motion. However, for the sake of investigation a quadratic term is added to the Lagrange multiplier interpolation. Hence one may write

$$\boldsymbol{G} = \begin{bmatrix} \frac{1}{L} & 0 & 0 & 0 \\ 0 & 1 & x' & x'^2 \end{bmatrix} , \tag{6-47}$$

which gives, substituting back into equation (2-19),

$$\boldsymbol{C} = \begin{bmatrix} -1 & 0 & 0 & 1 & 0 & 0 \\ 0 & 0 & -1 & 0 & 0 & 1 \\ 0 & \frac{1}{L} & 0 & 0 & -\frac{1}{L} & 1 \\ 0 & \frac{1}{L} & \frac{1}{6} & 0 & -\frac{1}{L} & \frac{5}{6} \end{bmatrix} . \tag{6-48}$$

It can be seen that the incorporation of a quadratic term furnished a linearly dependent constraint, since the fourth line is equal to the third minus the second divided by six. In other words, the inclusion of a quadratic term added no additional information on the constraints.

It's interesting to show that different interpolation functions generates different constraints and different physical meaning of discrete Lagrange multipliers. Namely, the Lagrange multiplier function for $\kappa = 0$ is given interpolated by

$$\gamma_\kappa = \mu_2 + x'\mu_3 \,. \tag{6-49}$$

If the function is rewritten on different basis such as

$$\widetilde{\gamma}_\kappa = \left(1 - \frac{x'}{L}\right)\widetilde{\mu}_2 + \frac{x'}{L}\widetilde{\mu}_3 \,, \tag{6-50}$$

This function is of course linear, and a relationship between the parameters on each function can be found as $\widetilde{\mu}_2 = \mu_2$ and $\widetilde{\mu}_3 = \mu_3 L + \mu_2$. Thus, the weighting function is the same, but written through different interpolation (basis) functions. Therefore, one may write

$$\boldsymbol{G} = \begin{bmatrix} 1 & 0 & 0 \\ 0 & 1 - \frac{x'}{L} & \frac{x'}{L} \end{bmatrix} , \tag{6-51}$$

which gives, substituting back into equation (2-19),

$$\boldsymbol{C} = \begin{bmatrix} -1 & 0 & 0 & 1 & 0 & 0 \\ 0 & -\frac{1}{L} & -1 & 0 & \frac{1}{L} & 0 \\ 0 & \frac{1}{L} & 0 & 0 & -\frac{1}{L} & 1 \end{bmatrix} . \tag{6-52}$$

It can be noticed that the two last lines on equation (6-45) and the two last lines on equation (6-52) are linearly dependent. In other words, the constraints found are the same but only written in a different manner.

The physical interpretation of the discrete Lagrange multiplier also change. While μ_2 and μ_3 are, respectively, the bending moment and shear force at the beginning of the member, $\widetilde{\mu}_2$ and $\widetilde{\mu}_3$ are the bending moment on each of the end nodes of the member. In other words, changing the interpolation of the Lagrange multiplier function changes how and in term of which parameters the bending moment diagram is expressed.

This formulation can be used to model frame members with node liberation, such as hinges, as well. This can be achieved by defining shape functions according to the prescribed nodal liberation and carrying out the same procedure to find the corresponding matrices.

6.3 Structural Analysis Formulation

The formulation more commonly used in structural analysis is based on the concept of kinematic incidence of nodal displacements and rotations on local axis, depicted in Figure 6.5 into a natural system, which captures the essence of possible deformations of a frame element. The natural system must be in equilibrium, hence a statically determined structure is used to model its behavior.

The natural system chosen consists of the supported beam shown in Figure 6.6. Other choices are also possible, as illustrated in Figure 6.7. Although ϵ_1, ϵ_2, and ϵ_3, in Figure 6.6, are displacements and rotations, they are treated as strains in this formulation, since the actual strains of beam theory within the element can be calculated after them as

$$\epsilon^a_{xx} = \frac{\epsilon_1}{L} , \tag{6-53}$$

$$\kappa = \left[\frac{2\,(2L - 3x')}{L^2}\right] \epsilon_2 - \left[\frac{2\,(L - 3x')}{L^2}\right] \epsilon_3 . \tag{6-54}$$

Therefore, the strain vector is given by

$$\boldsymbol{\epsilon} = \begin{Bmatrix} \epsilon_1 \\ \epsilon_2 \\ \epsilon_3 \end{Bmatrix} . \tag{6-55}$$

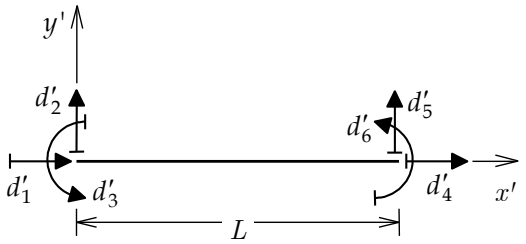

(a) Nodal displacements.

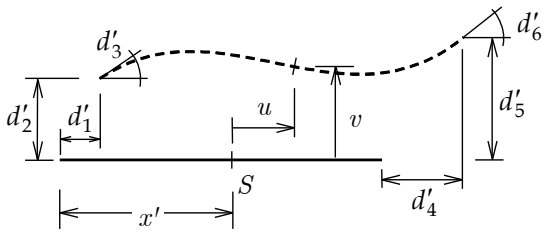

(b) Deformed configuration.

Figure 6.5: Nodal displacements of frame element.

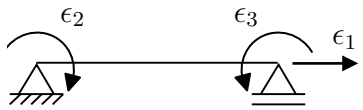

Figure 6.6: Frame element natural system displacements.

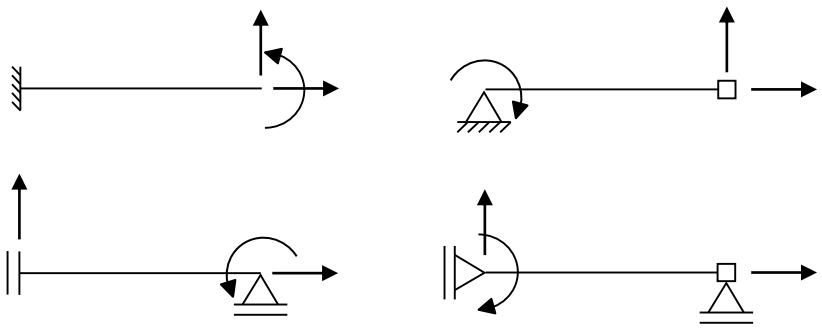

Figure 6.7: Alternative natural systems.

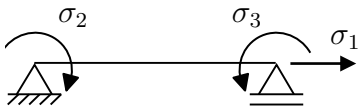

Figure 6.8: Frame element natural system forces.

Similarly, the stress vector of this approach is the static correspondents of ϵ_1, ϵ_2, and ϵ_3, which are σ_1, σ_2, and σ_3, or in matrix form

$$\boldsymbol{\sigma} = \begin{Bmatrix} \sigma_1 \\ \sigma_2 \\ \sigma_3 \end{Bmatrix} . \tag{6-56}$$

Which are actually forces and moments applied at the nodes, as shown in Figure 6.8. The actual stress resultants can be calculated as

$$N = \sigma_1 \, , \tag{6-57}$$

$$M = \left(1 - \frac{x'}{L}\right)\sigma_2 + \frac{x'}{L}\sigma_3 \, . \tag{6-58}$$

The stiffness relationship between the forces σ_1, σ_2, and σ_3 and the displacements ϵ_1, ϵ_2, and ϵ_3 plays the role of constitutive equation in this formulation, and it is given by

$$\boldsymbol{D} = \begin{bmatrix} \frac{EA}{L} & 0 & 0 \\ 0 & \frac{4EI}{L} & -\frac{2EI}{L} \\ 0 & -\frac{2EI}{L} & \frac{4EI}{L} \end{bmatrix} . \tag{6-59}$$

Therefore, the only ingredient missing for the complete definition of the frame element is the $\boldsymbol{B}$ matrix. As in equation (2-11) it must relate $\boldsymbol{\epsilon}$ to $\boldsymbol{d}$. In this approach, $\boldsymbol{\epsilon}$ is, as aforementioned, a displacement vector so the $\boldsymbol{B}$ matrix will be incidence matrix. The calculation of this matrix is carried out by applying a nodal displacement equal to one and measuring the correspondent displacement in the natural system, as illustrated in Figure 6.9. The final matrix is given by

$$\boldsymbol{B} = \begin{bmatrix} -1 & 0 & 0 & 1 & 0 & 0 \\ 0 & -\frac{1}{L} & -1 & 0 & \frac{1}{L} & 0 \\ 0 & \frac{1}{L} & 0 & 0 & -\frac{1}{L} & 1 \end{bmatrix} . \tag{6-60}$$

Using this formulation, the inextensible behavior may be modeled taking

$$\boldsymbol{A} = \begin{bmatrix} 1 & 0 & 0 \end{bmatrix} , \tag{6-61}$$

$$\boldsymbol{e} = \begin{Bmatrix} 0 \end{Bmatrix} . \tag{6-62}$$

While a frame element can be modeled with

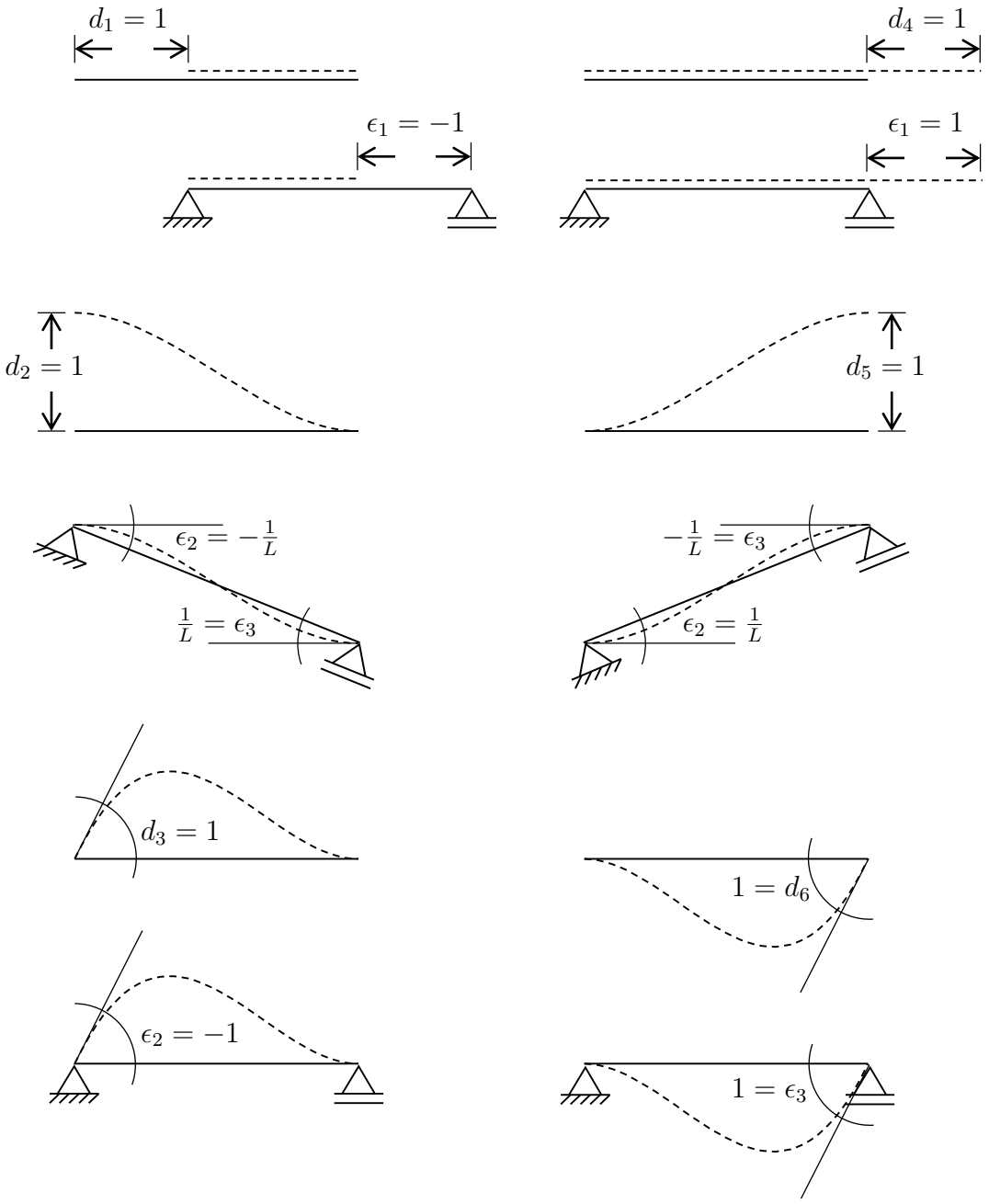

Figure 6.9: Frame element nodal to natural system displacements.

$$\boldsymbol{A} = \begin{bmatrix} 1 & 0 & 0 \\ 0 & 1 & 0 \\ 0 & 0 & 1 \end{bmatrix}, \tag{6-63}$$

$$\boldsymbol{e} = \begin{Bmatrix} 0 \\ 0 \\ 0 \end{Bmatrix}. \tag{6-64}$$

This formulation is preferable than the direct finite element approach for frame members since the formulation of constraints is more direct, does not requires additional integration, and does not generate linear dependent strain constraints at the element level. Furthermore, the formulation for end liberations is more straightforward than in the finite element approach for frame members. In Section 6.4 analysis of simple frames are performed to furnish a deep understanding of the methodology and the cases in which linear dependent constraints appears.

6.4 Frame Applications

This chapter presents the application of the proposed methodology to two simple frames to elucidate some aspects afore discussed. The first example, on Section 6.4.1, enlightens local to global transformation of constraint equations, assemblage of global constraint matrix and the calculation of internal forces. The second example, on Section 6.4.2, is mainly useful for perceiving how redundant constraints appears and how they affect the solution and the determination of internal forces.

6.4.1 Simple frame

Figure 6.10 shows a simple frame with inextensible columns and a rigid beam subjected to a described displacement ρ. The bending formulation of the columns neglects shear deformation. This example is used to illustrate these constraint relations in local and global coordinate systems.

The local constraint relations of members of the simple frame in Fig-

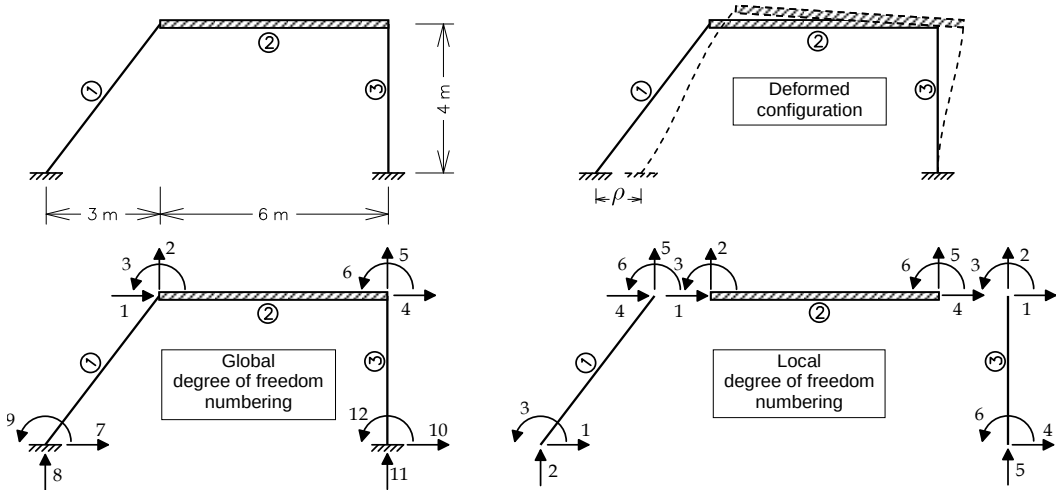

Figure 6.10: Simple frame with inextensible columns and rigid beam.

ure 6.10 in the global system are, for members 1, 2, and 3, respectively:

$$\boldsymbol{C}^1 = \begin{bmatrix} -0.6 & -0.8 & 0 & 0.6 & 0.8 & 0 \end{bmatrix}, \tag{6-65}$$

$$\boldsymbol{C}^2 = \begin{bmatrix} -1 & 0 & 0 & 1 & 0 & 0 \\ 0 & -\frac{1}{6} & -1 & 0 & \frac{1}{6} & 0 \\ 0 & \frac{1}{6} & 0 & 0 & -\frac{1}{6} & 1 \end{bmatrix}, \tag{6-66}$$

$$\boldsymbol{C}^3 = \begin{bmatrix} 0 & 1 & 0 & 0 & -1 & 0 \end{bmatrix}. \tag{6-67}$$

To assemble the global constraint matrix, it is defined a *stack vector*, for each constrained member, that relates local to global constraint numbering. For example, the stack vectors of the frame of Figure 6.10 are:

$$\boldsymbol{s}^1 = \begin{Bmatrix} 1 \end{Bmatrix}, \tag{6-68}$$

$$\boldsymbol{s}^2 = \begin{Bmatrix} 2 & 3 & 4 \end{Bmatrix}, \tag{6-69}$$

$$\boldsymbol{s}^3 = \begin{Bmatrix} 5 \end{Bmatrix}, \tag{6-70}$$

in which, $\boldsymbol{s}^m$ is the stack vector of member m. For members 1 and 3, the stack vectors are of dimension one as they are inextensible members, with only one constraint. On the other hand, the stack vector of rigid member 2 has dimension 3.

The stack vectors are used to assemble the global constraint matrix in the following way:

$$\hat{C}_{s_i^m, g_j^m} = c_{i,j}^m, \tag{6-71}$$

in which, $\hat{\boldsymbol{C}}$ is the global constraint matrix before handling boundary conditions; $m = 1, \ldots,$ number of members; $i = 1, \ldots,$ number of constraints; $j = 1, \ldots,$ number of degrees of freedom; and $\boldsymbol{g}^m$ is the gather vector of mem-

ber m, the same used in the global stiffness matrix assembling.

In the example of Figure 6.10, from the local and global numbering, the gather vectors of the members of this frame model are:

$$\boldsymbol{g}^1 = \begin{Bmatrix} 7 & 8 & 9 & 1 & 2 & 3 \end{Bmatrix}, \tag{6-72}$$

$$\boldsymbol{g}^2 = \begin{Bmatrix} 1 & 2 & 3 & 4 & 5 & 6 \end{Bmatrix}, \tag{6-73}$$

$$\boldsymbol{g}^3 = \begin{Bmatrix} 4 & 5 & 6 & 10 & 11 & 12 \end{Bmatrix}, \tag{6-74}$$

For the simple frame of Figure 6.10, the matrix $\hat{\boldsymbol{C}}$ is:

$$\hat{\boldsymbol{C}} = \begin{bmatrix} 0.6 & 0.8 & 0 & 0 & 0 & 0 & -0.6 & -0.8 & 0 & 0 & 0 & 0 \\ -1 & 0 & 0 & 1 & 0 & 0 & 0 & 0 & 0 & 0 & 0 & 0 \\ 0 & -\frac{1}{6} & -1 & 0 & \frac{1}{6} & 0 & 0 & 0 & 0 & 0 & 0 & 0 \\ 0 & \frac{1}{6} & 0 & 0 & -\frac{1}{6} & 1 & 0 & 0 & 0 & 0 & 0 & 0 \\ 0 & 0 & 0 & 0 & 1 & 0 & 0 & 0 & 0 & 0 & -1 & 0 \end{bmatrix}. \tag{6-75}$$

In the example of Figure 6.10, after considering the essential boundary conditions, as described in the equation (2-21), resulting global constraint matrix is:

$$\boldsymbol{C} = \begin{bmatrix} 0.6 & 0.8 & 0 & 0 & 0 & 0 \\ -1 & 0 & 0 & 1 & 0 & 0 \\ 0 & -\frac{1}{6} & -1 & 0 & \frac{1}{6} & 0 \\ 0 & \frac{1}{6} & 0 & 0 & -\frac{1}{6} & 1 \\ 0 & 0 & 0 & 0 & 1 & 0 \end{bmatrix}, \tag{6-76}$$

and the global constraint vector is:

$$\boldsymbol{q} = -\begin{bmatrix} -0.6 & -0.8 & 0 & 0 & 0 & 0 \\ 0 & 0 & 0 & 0 & 0 & 0 \\ 0 & 0 & 0 & 0 & 0 & 0 \\ 0 & 0 & 0 & 0 & 0 & 0 \\ 0 & 0 & 0 & 0 & -1 & 0 \end{bmatrix} \begin{Bmatrix} \rho \\ 0 \\ 0 \\ 0 \\ 0 \\ 0 \end{Bmatrix} = \begin{Bmatrix} 0.6\rho \\ 0 \\ 0 \\ 0 \\ 0 \\ 0 \end{Bmatrix} \tag{6-77}$$

Although there is no redundant constraint in this frame, the rref is carried out to generalize the procedure considering redundant constraints. The reduced constraint matrix $\boldsymbol{H}$, obtained from equation (3-10) is

$$\boldsymbol{H} = \begin{bmatrix} 1 & 0 & 0 & 0 & 0 & -8 \\ 0 & 1 & 0 & 0 & 0 & 6 \\ 0 & 0 & 1 & 0 & 0 & -1 \\ 0 & 0 & 0 & 1 & 0 & -8 \\ 0 & 0 & 0 & 0 & 1 & 0 \end{bmatrix}. \tag{6-78}$$

The corresponding $\boldsymbol{Z}$ matrix is

$$\boldsymbol{Z} = \begin{bmatrix} \frac{5}{3} & 0 & 0 & \frac{4}{3} & -\frac{4}{3} \\ 0 & 0 & 0 & -1 & 1 \\ 0 & 0 & -\frac{1}{6} & \frac{1}{6} & 0 \\ \frac{5}{3} & 1 & 0 & \frac{4}{3} & -\frac{4}{3} \\ 0 & 0 & 0 & 0 & 1 \end{bmatrix}, \tag{6-79}$$

which is used to find the constraint vector of the reduced problem, from equation (3-11):

$$\boldsymbol{p} = \boldsymbol{Z}\boldsymbol{q} = \begin{Bmatrix} \rho \\ 0 \\ 0 \\ \rho \\ 0 \end{Bmatrix}. \tag{6-80}$$

The solution of the constraint problem gives rise to the following Lagrange multipliers (see equation (3-9)):

$$\boldsymbol{\lambda} = \begin{Bmatrix} EI\rho/19 \\ -3EI\rho/76 \\ 10EI\rho/57 \\ -103EI\rho/1216 \\ 0 \end{Bmatrix}. \tag{6-81}$$

From this result, using equation (3-8), the displacement vector of the constrained model is:

$$\boldsymbol{d} = \begin{Bmatrix} 32\rho/57 \\ 25\rho/76 \\ -25\rho/456 \\ 32\rho/57 \\ 0 \\ -25\rho/456 \end{Bmatrix}, \tag{6-82}$$

whose physical interpretation is depicted in Figure 6.11.

Since this frame does not present redundant constraints, matrix $\boldsymbol{S}$ in equation (3-20) does not exist. Therefore, the Lagrange multipliers are:

$$\boldsymbol{\mu} = \boldsymbol{Z}^{\mathsf{T}}\boldsymbol{\lambda} = \begin{Bmatrix} -65EI\rho/1216 \\ -103EI\rho/1216 \\ -5EI\rho/171 \\ 71EI\rho/2736 \\ EI\rho/304 \end{Bmatrix}. \tag{6-83}$$

Member internal forces of this frame are obtained from Eq. (76). The resulting member internal force vectors, $\boldsymbol{f}^1$, $\boldsymbol{f}^2$, $\boldsymbol{f}^3$ are shown in the sequel:

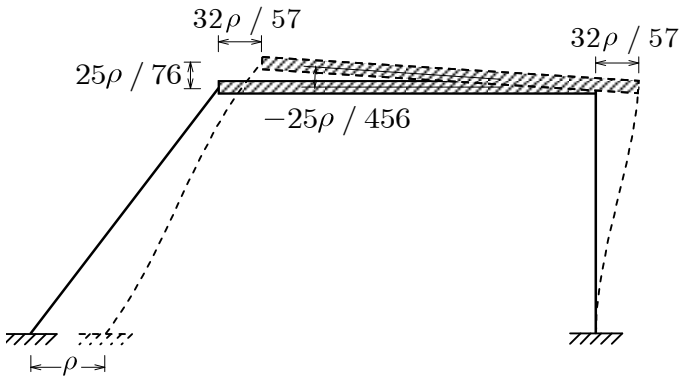

Figure 6.11: Physical interpretation of the displacement vector of simple frame example.

$$
\begin{aligned}
\boldsymbol{f}^1 &= \boldsymbol{K}^1\boldsymbol{d}^1 + \boldsymbol{C}^{1^{\mathsf{T}}}\boldsymbol{\mu}^1 \\
&= \boldsymbol{K}^1 \begin{Bmatrix} 3\rho/5 \\ -4\rho/5 \\ 0 \\ 3\rho/5 \\ -287\rho/1140 \\ -25\rho/456 \end{Bmatrix} + \begin{bmatrix} -1 \\ 0 \\ 0 \\ 1 \\ 0 \\ 0 \end{bmatrix} \{-65EI\rho/1216\} \\
&= \begin{Bmatrix} 65EI\rho/1216 \\ -5EI\rho/76 \\ -35EI\rho/228 \\ -65EI\rho/1216 \\ 5EI\rho/76 \\ -10EI\rho/57 \end{Bmatrix},
\end{aligned}
\tag{6-84}
$$

$$
\begin{aligned}
\boldsymbol{f}^2 &= \boldsymbol{K}^2\boldsymbol{d}^2 + \boldsymbol{C}^{2\mathsf{T}}\boldsymbol{\mu}^2 \\
&= \boldsymbol{K}^2 \begin{Bmatrix} 32\rho/57 \\ 25\rho/76 \\ -25\rho/456 \\ 32\rho/57 \\ 0 \\ -25\rho/456 \end{Bmatrix} + \begin{bmatrix} -1 & 0 & 0 \\ 0 & -1 & -1 \\ 0 & -6 & 0 \\ 1 & 0 & 0 \\ 0 & 1 & 1 \\ 0 & 0 & -6 \end{bmatrix} \begin{Bmatrix} -103EI\rho/1216 \\ -5EI\rho/171 \\ 71EI\rho/2736 \end{Bmatrix} \\
&= \begin{Bmatrix} 103EI\rho/1216 \\ EI\rho/304 \\ 10EI\rho/57 \\ -103EI\rho/1216 \\ -EI\rho/304 \\ -71EI\rho/456 \end{Bmatrix},
\end{aligned}
\tag{6-85}
$$

$$
\begin{aligned}
\boldsymbol{f}^3 &= \boldsymbol{K}^3\boldsymbol{d}^3 + \boldsymbol{C}^{3\mathsf{T}}\boldsymbol{\mu}^3 \\
&= \boldsymbol{K}^3 \begin{Bmatrix} 0 \\ 32\rho/57 \\ -25\rho/456 \\ 0 \\ 0 \\ 0 \end{Bmatrix} + \begin{bmatrix} -1 \\ 0 \\ 0 \\ 1 \\ 0 \\ 0 \end{bmatrix} \{EI\rho/304\} \\
&= \begin{Bmatrix} -EI\rho/304 \\ 103EI\rho/1216 \\ 71EI\rho/456 \\ EI\rho/304 \\ -103EI\rho/1216 \\ 167EI\rho/912 \end{Bmatrix}.
\end{aligned}
\tag{6-86}
$$

Physical representations of these internal forces are shown in Figure 6.12. To generate the diagrams of axial force, shear force, and bending moment shown in this figure, adequate numerical values for flexural rigidity, $EI = 2.432 \times 10^{-5}$ kNm^2, and for the prescribed displacement, $\rho = 0.003$ m, were used.

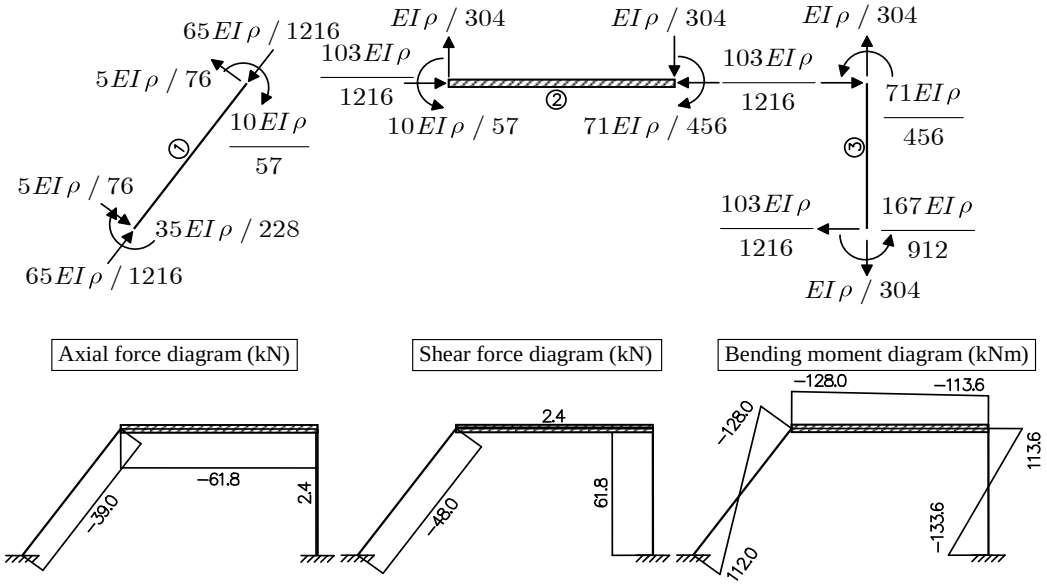

Figure 6.12: Member internal forces of simple frame ($EI = 2.432 \times 10^{-5}$kN m^2, $\rho = 0.003$m).

6.4.2
Frame with redundant constraints

Although the framework presented in Figure 6.10 could have been solved without the reduction of the constraint matrix to its reduced row echelon form, there are cases in which the constrained problem might have redundant constraints, which could make equation (3-9) to have infinite possible solutions. Additionally, problems with redundant constraints might become infeasible for a specific situation of prescribed displacements (settlements). To illustrate this, Figure 6.13 shows a simple frame with inextensible members. Member 1 provides the constraint $d_2 = 0$; member 2 furnishes the relation $d_1 = 0$; and member 3 also gives the equation $d_2 = 0$, which is a redundant information. That may be seen at the global constraint matrix

$$\boldsymbol{C} = \begin{bmatrix} 0 & 1 & 0 \\ 1 & 0 & 0 \\ 0 & -1 & 0 \end{bmatrix}, \tag{6-87}$$

in which, the first and third rows are linearly dependent.

In spite of this redundancy, this problem has a solution for the displacement vector of the type $\boldsymbol{d} = \begin{Bmatrix} 0 & 0 & \alpha \end{Bmatrix}$, in which α (rotation of the central node) may be determined through equation (3-1). However, if there were a prescribed vertical displacement ρ at the inferior node, the problem would be inconsistent with the inextensible member hypothesis, since the superior node has no prescribed displacement. The described condition reflects to the

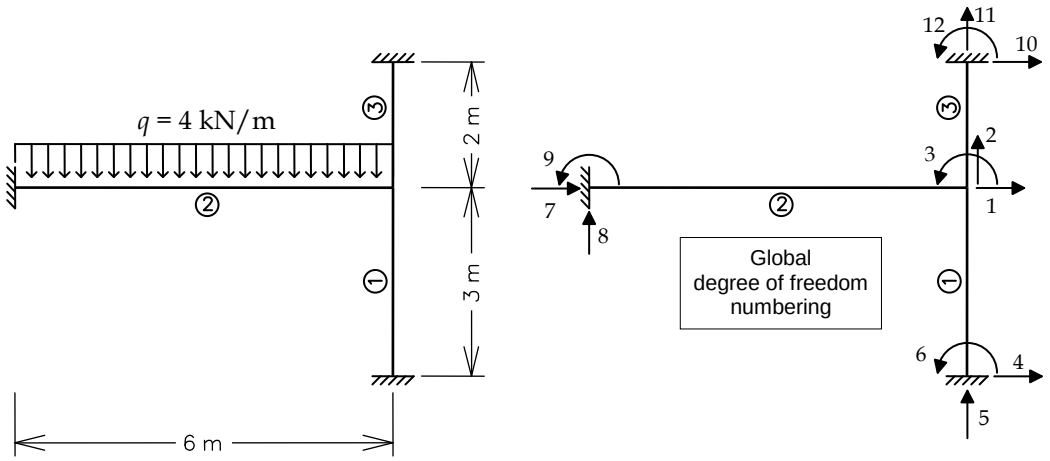

Figure 6.13: Frame with redundant constraints.

right-hand side given as

$$\boldsymbol{q} = \begin{Bmatrix} \rho \\ 0 \\ 0 \end{Bmatrix} . \tag{6-88}$$

It is clear that there is no solution for $\boldsymbol{Cd} = \boldsymbol{q}$ under this condition. Thus, the problem is infeasible. However, some constraints matrix are more complicated and such visualization is not possible directly. Therefore, the criterion described at Chapter 3 is needed, since it is easily applied.

The rref of the augmented matrix $\begin{bmatrix} \boldsymbol{C} & \boldsymbol{I} \end{bmatrix}$ is

$$\begin{bmatrix} \boldsymbol{H} & \boldsymbol{Z} \\ \boldsymbol{0} & \boldsymbol{S} \end{bmatrix} = \left[\begin{array}{ccc:ccc} 1 & 0 & 0 & 0 & 1 & 0 \\ 0 & 1 & 0 & 0 & 0 & -1 \\ \hdashline 0 & 0 & 0 & 1 & 0 & 1 \end{array}\right] . \tag{6-89}$$

Considering the prescribed displacement condition equations (3-11) and (3-12) become

$$\boldsymbol{p} = \begin{Bmatrix} 0 & 0 \end{Bmatrix}^{\mathsf{T}} , \tag{6-90}$$

$$\boldsymbol{y} = \begin{Bmatrix} \rho \end{Bmatrix} . \tag{6-91}$$

Thereby, equation (3-3) is only verified if $\rho = 0$.

Continuing the solution of the problem at Figure 6.13, considering zero prescribed displacement, the equivalent nodal force vector is given by

$$\boldsymbol{f} = \begin{Bmatrix} 0 \\ -\frac{qL}{2} \\ \frac{qL^2}{12} \end{Bmatrix} = q \begin{Bmatrix} 0 \\ -3 \\ 3 \end{Bmatrix} . \tag{6-92}$$

Calculating the displacement vector gives

$$\boldsymbol{d} = \begin{Bmatrix} 0 \\ 0 \\ \frac{3q}{4EI} \end{Bmatrix} . \tag{6-93}$$

The resulting nodal internal force vector is:

$$\boldsymbol{K}\boldsymbol{d} = q \begin{Bmatrix} -\frac{5}{8} \\ -\frac{1}{8} \\ 3 \end{Bmatrix} , \tag{6-94}$$

which is not in equilibrium with the nodal external force vector.

In fact, the equilibrium is satisfied considering the nodal constraint force vector:

$$\boldsymbol{C}^{\mathsf{T}}\boldsymbol{\mu} = \begin{Bmatrix} \mu_2 \\ \mu_1 - \mu_3 \\ 0 \end{Bmatrix} , \tag{6-95}$$

as shown in the modified equilibrium equation (3-19), which for the example of equation (3-19) reduces to:

$$q \begin{Bmatrix} -\frac{5}{8} \\ -\frac{1}{8} \\ 3 \end{Bmatrix} - q \begin{Bmatrix} 0 \\ -3 \\ 3 \end{Bmatrix} + \begin{Bmatrix} \mu_2 \\ \mu_1 - \mu_3 \\ 0 \end{Bmatrix} = \{0\} . \tag{6-96}$$

From equation (6-96), $\mu_2 = q\frac{5}{8}$ and $\mu_1 - \mu_3 = -q\frac{23}{8}$. Therefore, as expected, there are infinite solutions for μ_1 and μ_3, since the redundant constraints are associated to members 1 and 3.

On the other hand, the solution of the reduced problem, equation (3-4), given by equation (3-9) has a unique solution. The modified equilibrium equation (3-6) for the problem of Figure 6.13 considers the nodal constraint force vector given by:

$$\boldsymbol{H}^{\mathsf{T}}\boldsymbol{\lambda} = \begin{Bmatrix} \lambda_1 \\ \lambda_2 \\ 0 \end{Bmatrix} , \tag{6-97}$$

resulting in the following values for the Lagrange multipliers of the reduced problem: $\lambda_1 = q\frac{5}{8}$ and $\lambda_2 = -q\frac{23}{8}$.

Using equation (3-20) the Lagrange multipliers of the original problem are given by

$$\begin{aligned} \boldsymbol{\mu} &= \begin{bmatrix} 0 & 0 \\ 1 & 0 \\ 0 & -1 \end{bmatrix} \begin{Bmatrix} 5/8 \\ -23/8 \end{Bmatrix} q + \begin{bmatrix} 1 \\ 0 \\ 1 \end{bmatrix} \boldsymbol{\alpha} \\ &= \begin{Bmatrix} 0 \\ 5/8 \\ 23/8 \end{Bmatrix} q + \begin{Bmatrix} \alpha_1 \\ 0 \\ \alpha_1 \end{Bmatrix} . \end{aligned} \tag{6-98}$$

It is worth pointing out that the for the example of Figure 6.13 vector $\boldsymbol{\alpha}$ is a scalar α_1 since there is only one redundant constraint.

Analyzing the global equilibrium equation,

$$\boldsymbol{K}\boldsymbol{d} + \boldsymbol{C}^{\mathsf{T}}\boldsymbol{\mu} = \boldsymbol{K}\boldsymbol{d} + \boldsymbol{C}^{\mathsf{T}}\left(\boldsymbol{Z}^{\mathsf{T}}\boldsymbol{\lambda} + \boldsymbol{S}^{\mathsf{T}}\boldsymbol{\alpha}\right) = \boldsymbol{f}\,, \tag{6-99}$$

of the structural model presented in Figure 6.13, for which the first term is given in equation (6-94) and the second is split into two

$$\boldsymbol{C}^{\mathsf{T}}\boldsymbol{\mu} = \boldsymbol{C}^{\mathsf{T}}\boldsymbol{Z}^{\mathsf{T}}\boldsymbol{\lambda} + \boldsymbol{C}^{\mathsf{T}}\boldsymbol{S}^{\mathsf{T}}\boldsymbol{\alpha}\,, \tag{6-100}$$

whose first evaluates to

$$\boldsymbol{C}^{\mathsf{T}}\boldsymbol{Z}^{\mathsf{T}}\boldsymbol{\lambda} = \begin{bmatrix} 0 & 1 & 0 \\ 1 & 0 & -1 \\ 0 & 0 & 0 \end{bmatrix} \begin{bmatrix} 0 & 0 \\ 1 & 0 \\ 0 & -1 \end{bmatrix} \begin{Bmatrix} \frac{5}{8} \\ -\frac{23}{8} \end{Bmatrix} q = \begin{Bmatrix} \frac{5}{8} \\ -\frac{23}{8} \\ 0 \end{Bmatrix} q\,, \tag{6-101}$$

while the second terms becomes

$$\boldsymbol{C}^{\mathsf{T}}\boldsymbol{S}^{\mathsf{T}}\boldsymbol{\alpha} = \begin{bmatrix} 0 & 1 & 0 \\ 1 & 0 & -1 \\ 0 & 0 & 0 \end{bmatrix} \begin{bmatrix} 1 \\ 0 \\ 1 \end{bmatrix} \alpha_1 = \begin{bmatrix} 0 \\ 0 \\ 0 \end{bmatrix} \alpha_1\,, \tag{6-102}$$

one can conclude that the global equilibrium matrix is satisfied for any value of $\boldsymbol{\alpha}$.

With the Lagrange multipliers on equation (6-98), the internal forces of member 1 may be written as

$$\boldsymbol{f}^1 = \begin{Bmatrix} 0 \\ 1 \\ 1 \\ 0 \\ -1 \\ 2 \end{Bmatrix} \frac{q}{2} + \begin{bmatrix} -1 \\ 0 \\ 0 \\ 1 \\ 0 \\ 0 \end{bmatrix} \alpha_1\,, \tag{6-103}$$

while the internal forces of member 2 are

$$\boldsymbol{f}^2 = \begin{Bmatrix} 0 \\ 1 \\ 2 \\ 0 \\ -1 \\ 4 \end{Bmatrix} \frac{q}{8} + \begin{bmatrix} -1 \\ 0 \\ 0 \\ 1 \\ 0 \\ 0 \end{bmatrix} \frac{5}{8} q\,, \tag{6-104}$$

and, lastly, the internal forces of member 3 are given by:

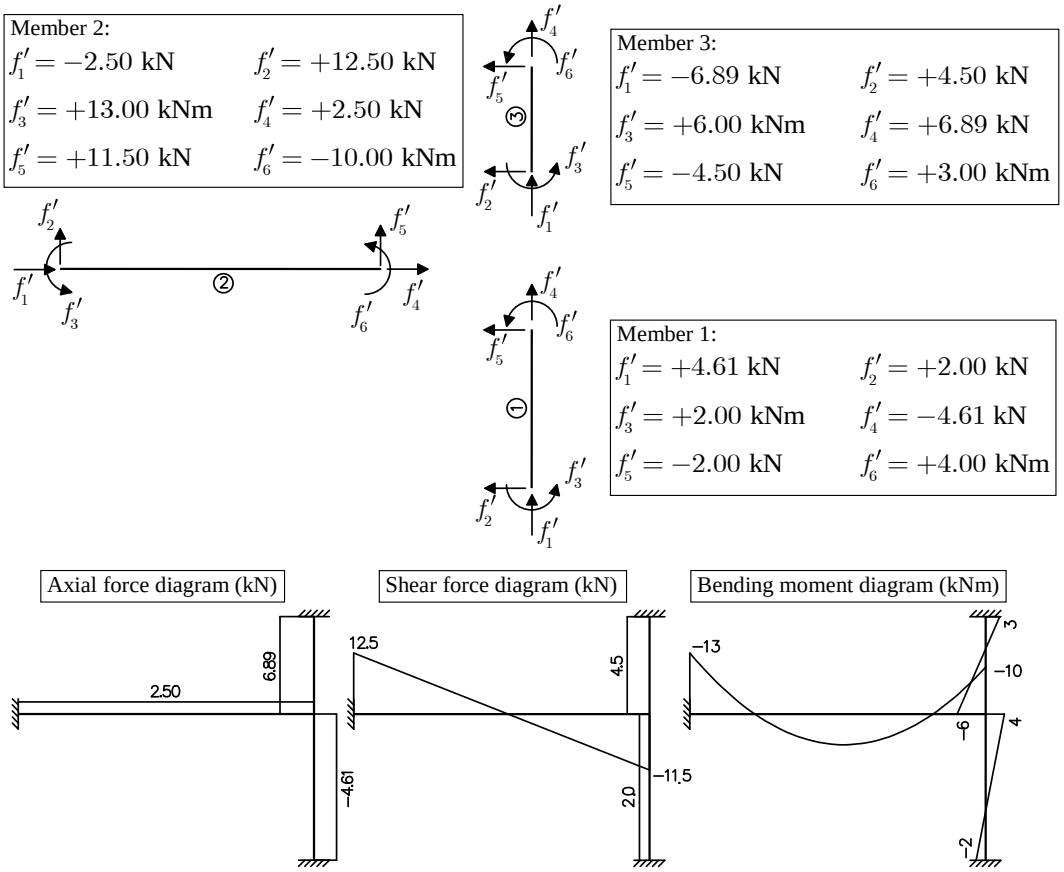

Figure 6.14: Internal forces in members of frame with redundant constraints.

$$\boldsymbol{f}^3 = \begin{Bmatrix} 0 \\ 3/2 \\ 1 \\ 0 \\ -3/2 \\ 2 \end{Bmatrix} \frac{3}{4}q + \begin{bmatrix} -1 \\ 0 \\ 0 \\ 1 \\ 0 \\ 0 \end{bmatrix} \left(\frac{23}{8}q + \alpha_1\right) \tag{6-105}$$

It can be seen in equations (6-103) and (6-105) that the axial forces on members 1 and 3 of the example of Figure 6.13 have infinite valid solutions, one for each value of parameter α_1. Therefore, vector $\boldsymbol{\alpha}$ changes the distribution of internal forces without disrupting the global equilibrium.

Applying the minimization procedure described in chapter 3 to the example in study, shown in Figure 6.13, one may find $\alpha_1 = -1.1523q$. Assuming $q = 4\text{kN/m}$, the internal forces of this example are shown in Figure 6.14.

7
Results

7.1
Partially rigid beam

This example comprises a beam of stiffness and length under a mid-span load. Moreover, half of its domain is rigid as shown in Figure 7.1. Shear deformation of the second beam half is neglected. Its solution is found using the penalty method to illustrate the numeral problems that may arise. Then the solution with the proposed Lagrange multiplier methodology is presented to validate its robustness.

The degrees of freedom used to model this structure are presented in Figure 7.1a: Δ (transversal displacement at mid spam) and θ (rotation of mid spam cross-section). Since this is a statically determinate model, shear force and bending moment responses are independent of the stiffness properties of the beam, as shown in Figures 7.1b and 7.1c, respectively.

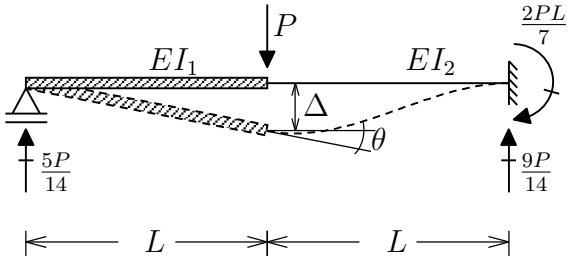

(a) Structural model.

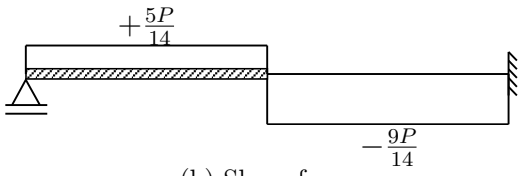

(b) Shear forces.

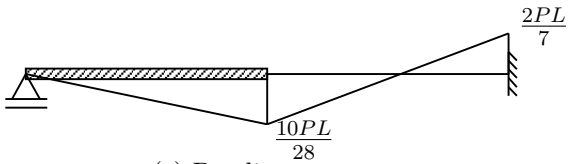

(c) Bending moment.

Figure 7.1: Partially rigid beam.

In the penalty method, a finite value, EI_1, for the flexural rigidity in the first half span is used. The flexural rigidity of the second half spam is EI_2, and the ratio between them is:

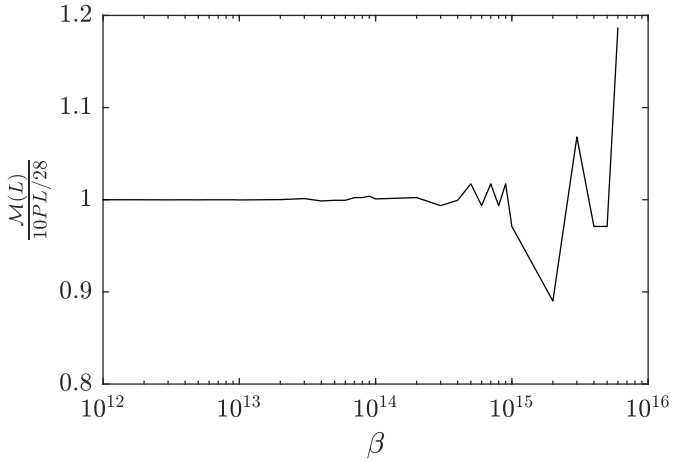

Figure 7.2: Semi-log graph of ratio β vs. normalized bending moment at mid span of beam.

$$\beta = \frac{EI_1}{EI_2}\,.$$

The resulting system of equilibrium equations of this problem is:

$$\frac{3EI_2}{L^2}\begin{bmatrix} \frac{4+\beta}{L} & 2-\beta \\ 2-\beta & \left(\frac{4}{3}+\beta\right)L \end{bmatrix}\begin{Bmatrix}\Delta\\ \theta\end{Bmatrix} = \begin{Bmatrix}P\\ 0\end{Bmatrix}\,.$$

After solving this system of equations, the bending moment at mid beam spam may be computed from:

$$\mathcal{M}\left(x=L\right) = \frac{2EI_2}{L^2}\left(3\Delta + 2\theta L\right)$$

Figure 7.2 depicts a graph, in semilog scale, relating the flexural rigidity ratio β with the ratio between the computed bending moment at mid spam and its analytical value $\mathcal{M}\left(L\right) = \frac{10}{28}PL$, assuming $L = 1\text{m}$, $P = 1\text{kN}$, and $EI_2 = 10^5\text{kN}\,\text{m}^2$. It can be seen in the graph of Figure 7.2 that for values of β greater than 10^{13} the numerical solution diverges, which demonstrates the instability of the penalty method.

The solution of this problem using the proposed Lagrange multiplier method assumes the same flexural rigidity for the unconstrained problem, hence no ill-condition issues arise in the solution of equilibrium equation. Thereafter, the solution found through the proposed Lagrange multiplier method does not presents numerical instabilities.

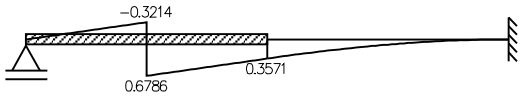

(a) Shear forces influence line.

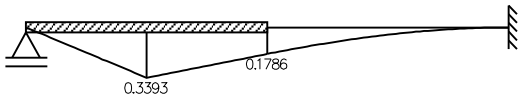

(b) Bending moment influence line.

Figure 7.3: Partially rigid beam.

7.2 Influence line

This examples sheds lights on the advantage of general treatment of strain constraints as in equation (2-7). To do so, a nonzero b vector example is provided. It may be useful on finding influence lines of bending moment and shear force through kinematic procedure. Shear force influence line of a section with local coordinate $x' = a$ within a member of length L may be modeled as

$$\boldsymbol{A} = \begin{bmatrix} 1 & 0 & 0 \\ 0 & a & L-a \\ 0 & 1 & -1 \end{bmatrix}, \ \boldsymbol{e} = \begin{Bmatrix} 0 \\ 1 \\ 0 \end{Bmatrix}.$$

While, the bending moment influence line may be modeled as

$$\boldsymbol{A} = \begin{bmatrix} 1 & 0 & 0 \\ 0 & 1 & 0 \\ 0 & 0 & 1 \end{bmatrix}, \ \boldsymbol{e} = \begin{Bmatrix} 0 \\ \frac{L-a}{L} \\ \frac{a}{L} \end{Bmatrix}.$$

The influence lines of shear force and bending moment for the beam model depicted on Figure 7.1a considering $a = 0.5$m (from left support) are illustrated in Figure 7.3.

7.3 Shear building

This example consists of a two-dimensional model of a 2-bay and 5-storey building with rigid floors and inextensible columns loaded by horizontal forces of 18 kN applied to each floor, as depicted in Figure 7.4. The properties of all members of the unconstrained model are $E = 24$GPa (elasticity modulus), $A = 750\text{cm}^2$ (cross-section area), and $I = 156250\text{cm}^4$ (cross-section moment of inertia). The columns of the constrained model maintain the same value of flexural rigidity EI and do not consider shear deformation.

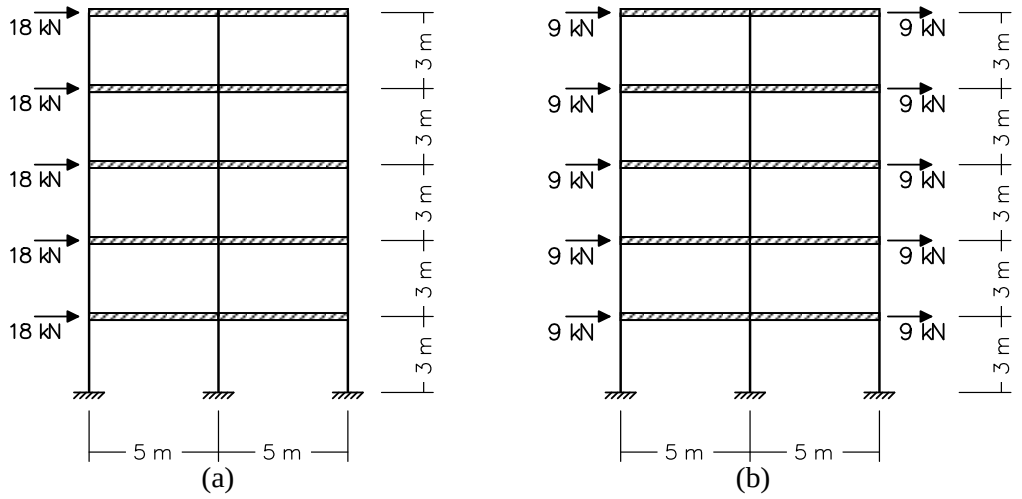

Figure 7.4: Shear building structural model with (a) asymmetric loading and (b) symmetric loading.

It should be noticed that this frame model has redundant constraints, since only two inextensible columns are needed to restrain the rotation of the rigid floor. Therefore, the axial deformation constraint of the third column is linearly dependent. Hence, the axial forces of these columns are determined using the methodology presented in Chapter 4. For this reason, the results of the unconstrained model are necessary.

To analyze the impact of the unconstrained model results, the loading in the shear building are considered in two different manners. Firstly, the loads are applied on the left-hand-side of the frame, hence asymmetrically, as illustrated in Figure 7.4(a). Secondly, the loads are symmetrically divided on each floor, as shown in Figure 7.4(b). Figure 7.5 shows the axial forces in all members of the unconstrained structural model considering asymmetric loading, in Figure 7.5(a), and symmetric loading, in Figure 7.5(b).

It may be observed in Figure 7.5 that the unconstrained model response for asymmetric loading is not symmetric. Consequently, the response of constrained model, axial forces shown in Figure 7.6, are symmetric only if the loading is symmetrically applied. Since the symmetric response is intuitively expected for the shear building model, the structural responses of displacements, shear forces, and bending moment are illustrated in Figure 7.7, considering symmetric loading. The dependency of the constrained response on the results of the unconstrained model might be a drawback of the proposed methodology.

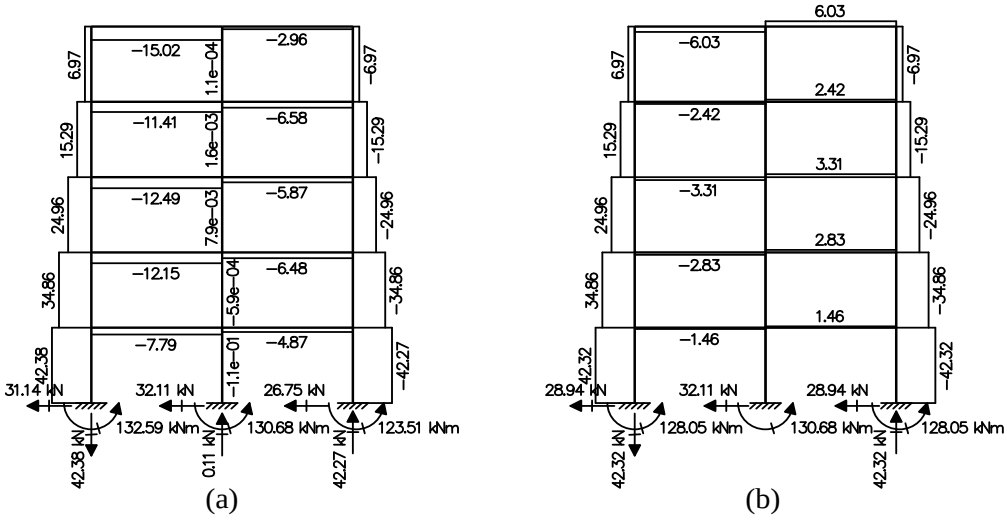

Figure 7.5: Shear building axial force diagram (kN) of unconstrained structural model: (a) Asymmetric loading, (b) Symmetric loading.

7.4 Asymmetric strip footing

An asymmetric strip footing under constant pressure $p = 1\text{kN/m}^2$ is herein analyzed. The soil material parameter are: Young modulus $E = 3\text{MPa}$ and Poisson ratio $\nu = 0.3$. The footing is considered rigid, but the soil should be free to deform transversally under the footing. This behavior is modeled with a constraint $\epsilon_{yy} = 0$ and a very low Young modulus $E = 1\text{kPa}$ for the footing, so that the displacement in the x-direction is practically free. The mesh discretization used is shown in Figure 7.8. The footing geometry and mesh is shown in detail in Figure 7.9.

The stress σ_{yy} of the footing is depicted in Figure 7.10 along its deformed configuration. It can be seen that the stress are successfully calculated.

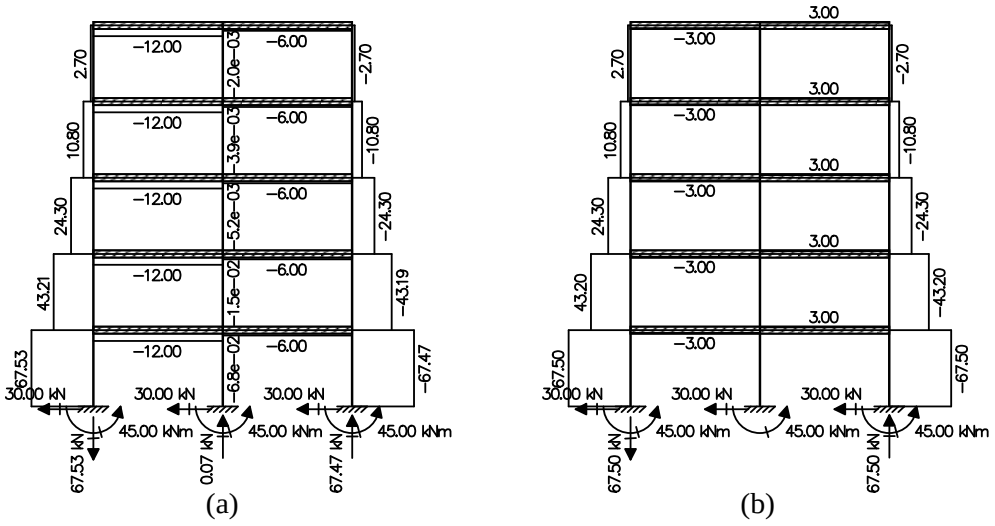

Figure 7.6: Shear building axial force diagram (kN) of constrained structural model: (a) Asymmetric loading, (b) Symmetric loading.

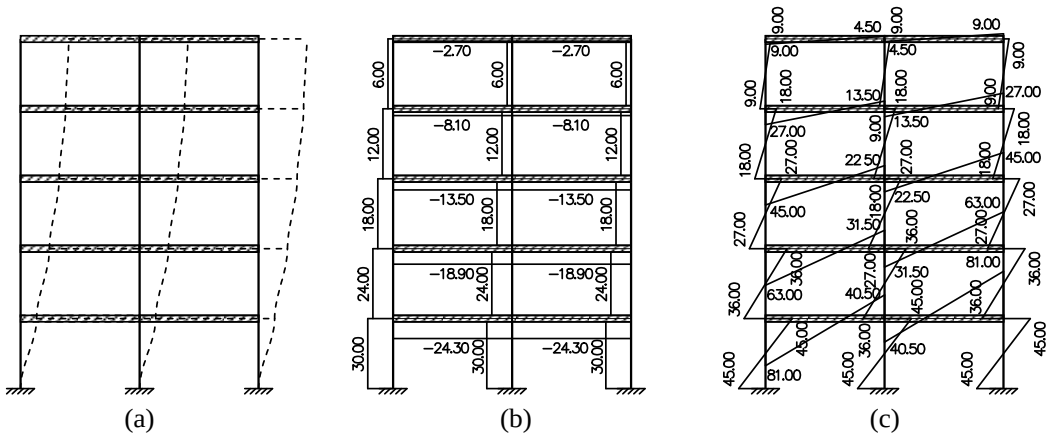

Figure 7.7: Shear building responses for symmetric loading: (a) deformed configuration (deformed factor = 6000), (b) shear force diagram (kN), and (c) bending moment diagram (kNm).

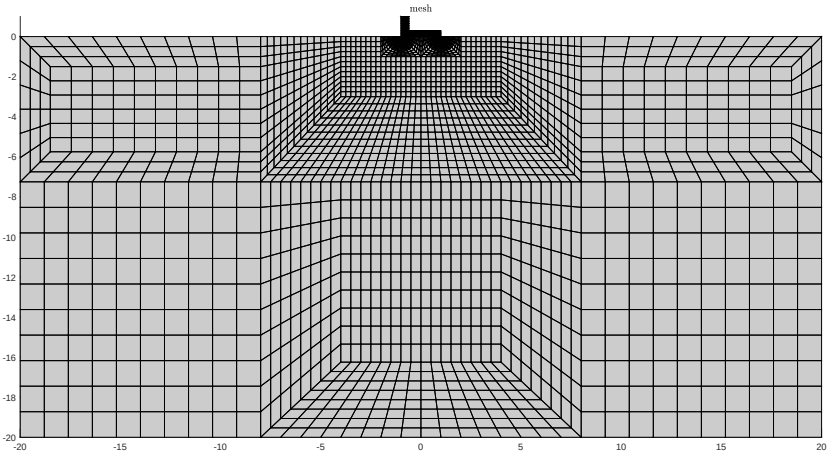

Figure 7.8: Strip footing geometry and mesh discretization.

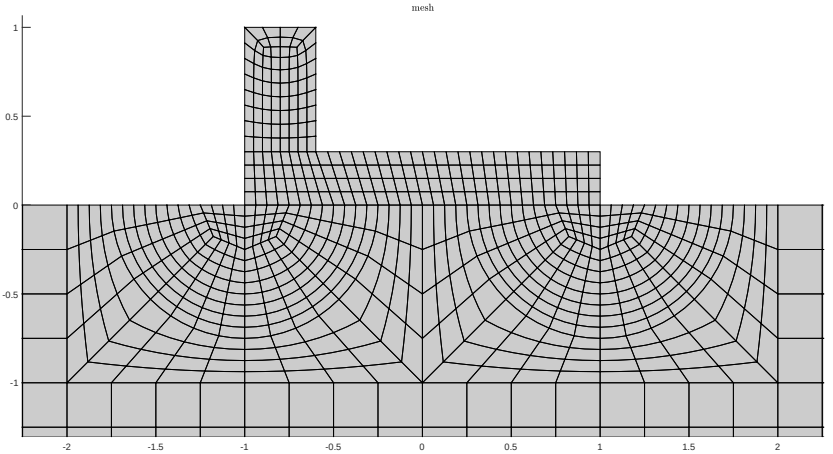

Figure 7.9: Strip footing geometry and mesh discretization – detail.

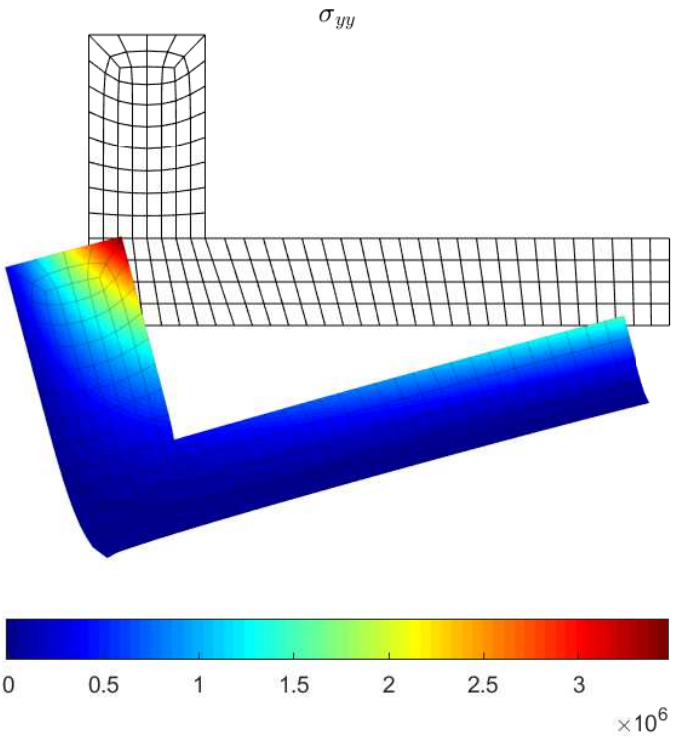

Figure 7.10: Stress σ_{yy} on the footing.

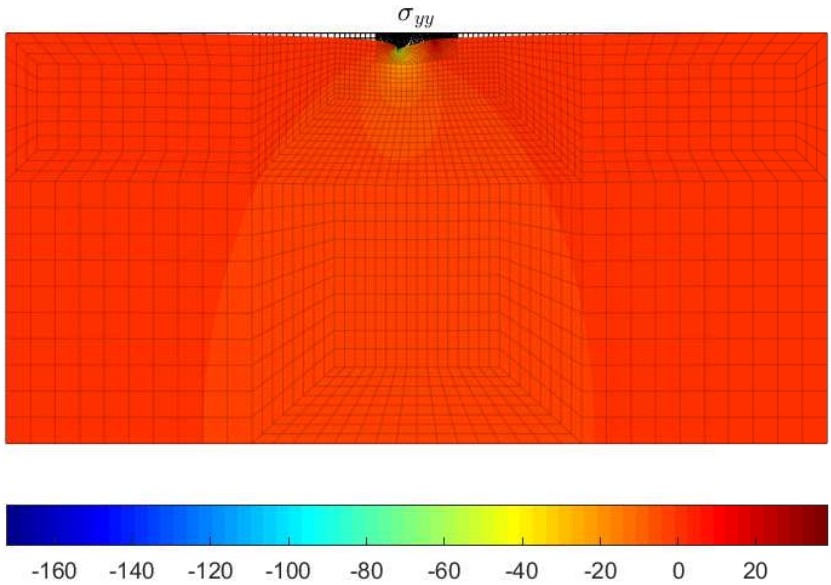

Figure 7.11: Stress σ_{yy} on the soil.

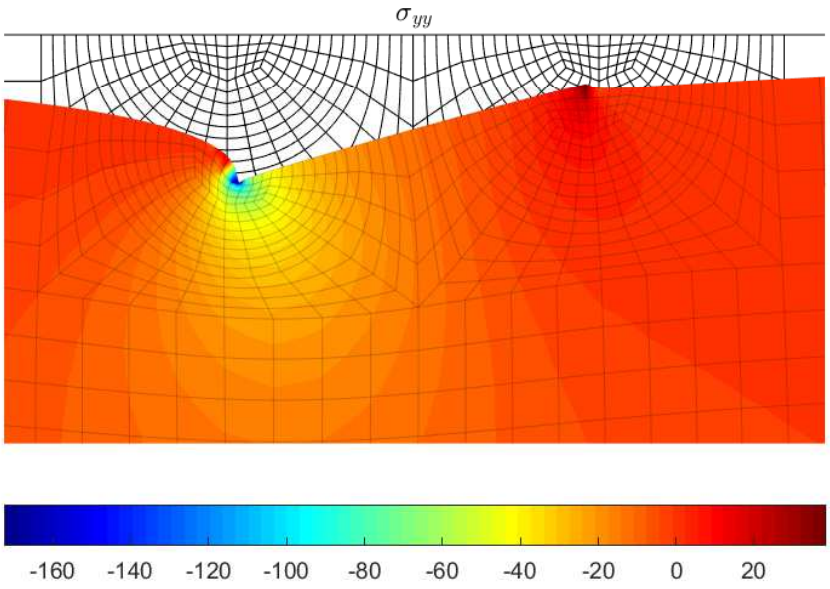

Figure 7.12: Stress σ_{yy} on the soil next to footing.

8
Conclusions

This work deals with the finite element method for structural analysis considering strain constraints, such as framed structures with inextensible and infinitely rigid member, i.e., with null axial and bending deformations. Rigid and inextensible members may be useful in educational software because they capture the essence of structural behavior with a reduced number of variables.

The proposed methodology considers structural member deformation constraints using Lagrange multipliers. It consists of adding strain constraints into the total potential energy minimization, leading to a quadratic programming problem. The solution gives rise to one Lagrange multiplier per constraint, which is essential for computing member internal forces. In addition, the adopted approach is suitable for computational implementation, since it preserves the generic characteristic of a matrix structural analysis: direct assemblage of element matrices to global model matrix.

However, there are situations in which the constraints of rigid and inextensible members can be redundant, resulting in infinite solutions for member internal forces. In these situations, it is not possible to determine the values of dependent Lagrange multipliers. The adopted solution to eliminate linearly dependent constraints and the associated Lagrange multipliers is to find the reduced row echelon form (rref) of the redundant global constraint matrix, reformulating the problem in terms of the reduced matrix.

There is still the problem of defining the internal forces of a redundant constraint problem. The solution is found by minimizing the difference between member internal forces of the constrained and the unconstrained models. For this, the reduced vector of Lagrange multipliers is augmented by adding to the particular solution any linear combination of vectors belonging to the kernel of matrix.

The dependency on an unconstrained response for obtaining internal forces in members of a constrained model may be a drawback of the proposed methodology. In fact, the results of the shear building example of Section 5.3 with the penalty method would not depend on symmetric or asymmetric loadings. One alternative that may be explored in the future would be to minimize the difference between the internal forces obtained by the proposed Lagrange multipliers method and the ones obtained by the penalty method. The problem with this is that the penalty method sometimes fails due to numerical problems.

The presented methodology is implemented in the educational software Ftool and will be available in its next distributed version. Future developments are related to finding constraint equations for influence lines of internal forces in cross-sections of infinitely rigid members. These influence lines correspond to the deformed configuration resulting from the application of unitary discontinuities of displacement or rotation at the target cross-section. In addition, the proposed methodology for considering frame member with deformation constraints is being extended for geometric non-linear analysis in Ftool.

As aforementioned the calculation of matrix $\boldsymbol{L}$ in equation (3-8) does not represent a computational hurdle since it is the same of multiple right hand side system of equations. On the other hand, the solution of equation (3-9) may be a significant overhead for highly constrained mesh discretization, since if is a system of equation of the order of the linear independent constraints. Additionally, one has to assemble and solve equation (4-6) which is in general less time consuming given that the number of redundant constraints is generally small. For the stress recovery processes, one small system of equations has to be solved. This is not considered overwhelming since it is on element level and involve solely the degrees of freedom of each element separately. The major observed computational drawback is the computation of the reduced row echelon form of the constraint matrix. Therefore, it can be observed in future works a methodology to circumvent that issue.

9
Bibliography

ABEL, J. F.; SHEPHARD, M. S. An algorithm for multipoint constraints in finite element analysis. **International Journal for Numerical Methods in Engineering**, John Wiley & Sons, Ltd, v. 14, n. 3, p. 464–467, jan 1979. ISSN 0029-5981. Cited in page 11.

BARLOW, J. Constraint relationships in linear and nonlinear finite element analyses. **International Journal for Numerical Methods in Engineering**, John Wiley & Sons, Ltd, v. 18, n. 4, p. 521–533, apr 1982. ISSN 0029-5981. Cited 2 times in pages 11 and 12.

BATHE, K. J. **Finite Element Procedures**. [S.l.]: Prentice Hall, 1996. Cited 2 times in pages 14 and 19.

COOK, R. D. et al. **Concept and Applications of Finite Element Analysis**. Fourth. Danvers, MA: John Wiley & Sons, 2002. 733 p. ISBN 978-0-471-35605-9. Cited 4 times in pages 11, 12, 14, and 19.

CURISKIS, J.; VALLIAPPAN, S. A solution algorithm for linear constraint equations in finite element analysis. **Computers & Structures**, Pergamon, v. 8, n. 1, p. 117–124, feb 1978. ISSN 0045-7949. Cited in page 11.

DUBOIS-PÈLERIN, Y.; PEGON, P. Linear constraints in object-oriented finite element programming. **Computer Methods in Applied Mechanics and Engineering**, North-Holland, v. 154, n. 1-2, p. 31–39, feb 1998. ISSN 0045-7825. Cited in page 12.

FELIPPA, C. A. Error analysis of penalty function techniques for constraint definition in linear algebraic systems. **International Journal for Numerical Methods in Engineering**, John Wiley & Sons, Ltd, v. 11, n. 4, p. 709–728, jan 1977. ISSN 0029-5981. Cited in page 12.

FELIPPA, C. A. **Introduction to Finite Element Methods, class notes of "Introduction to Finite Elements Methods (ASEN 5007) – Fall 2017, Department of Aerospace Engineering Sciences, University of Colorado at Boulder"**. 2017. Disponível em: <www.colorado.edu/engineering/CAS/courses.d/IFEM.d>. Cited 2 times in pages 11 and 12.

HOULSBY, G. T.; LIU, G.; AUGARDE, C. E. A tying scheme for imposing displacement constraints in finite element analysis. **Communications in Numerical Methods in Engineering**, John Wiley & Sons, Ltd, v. 16, n. 10, p. 721–732, oct 2000. ISSN 1069-8299. Cited in page 12.

KUHN, H. W.; TUCKER, A. Nonlinear Programming. **Proceedings of the Second Berkeley Symposium on Mathematical Statistics and Probability**, p. 481–492, 1951. ISSN 01605682. Disponível em: <http://projecteuclid.org/euclid.bsmsp/1200500249>. Cited in page 19.

MARTÍN, F.; BENAVENT-CLIMENT, A.; GALLEGO, R. A scheme for imposing constraints and improving conditioning of structural stiffness matrices. **International Journal for Numerical Methods in Biomedical Engineering**, John Wiley & Sons, Ltd, v. 26, n. 9, p. 1117–1124, sep 2010. ISSN 20407939. Cited 2 times in pages 11 and 12.

MCGUIRE, W.; GALLAGHER, R. H.; ZIEMIAN, R. D. **Matrix Structural Analysis**. 2nd. ed. [S.l.]: CreateSpace Independent Publishing Platform, 2014. 482 p. ISBN 978-0471129189. Cited in page 26.

MEYER, C. D. **Matrix analysis and applied linear algebra**. Philadelphia, PA: Society for Industrial and Applied Mathematics (SIAM), 2000. 718 p. ISBN 0898719518. Cited 2 times in pages 12 and 19.

NOCEDAL, J.; WRIGHT, S. J. J. **Numerical optimization**. 2nd. ed. [S.l.]: Springer, 2006. 664 p. ISSN 10969101. ISBN 9780387303031. Cited in page 18.

NOUR-OMID, B.; WRIGGERS, P. A note on the optimum choice for penalty parameters. **Communications in Applied Numerical Methods**, John Wiley & Sons, Ltd, v. 3, n. 6, p. 581–585, nov 1987. ISSN 0748-8025. Cited in page 12.

WEBB, J. P. Imposing linear constraints in finite-element analysis. **Communications in Applied Numerical Methods**, John Wiley & Sons, Ltd, v. 6, n. 6, p. 471–475, aug 1990. ISSN 0748-8025. Cited in page 11.

ZIENKIEWICZ, O. C.; TAYLOR, R. L.; ZHU, J. Z. **The Finite Element Method: Its Basis and Fundamentals**. 6th. ed. Burlington, MA: Elsevier Butterworth-Heinemann, 2013. 756 p. ISBN 0 7506 6320 0. Cited 3 times in pages 11, 14, and 19.